

Title: Organismal responses to extreme temperatures reduce coral reef biodiversity and functioning

Authors: Simon J. Brandl^{1,2,3,4*}†, Jacob L. Johansen^{5,6†}, Jordan M. Casey^{3,4}, Luke Tornabene⁷, Renato A. Morais^{8,9}, John A. Burt⁶

† indicates shared first authorship

***Corresponding author:** Simon J. Brandl, simonjbrandl@gmail.com,
(ORCID: 0000-0002-6649-2496)

Affiliations:

¹ Department of Biological Sciences, Simon Fraser University, Burnaby, BC, Canada

² CESAB - FRB, 5 Rue de l'École de Médecine, 34000, Montpellier, France

³ PSL Université Paris: CNRS-EPHE-UPVD USR3278 CRIOBE, Université de Perpignan, Perpignan, France

⁴ Laboratoire d'Excellence "CORAIL," Perpignan, France

⁵ Hawai'i Institute of Marine Biology, University of Hawai'i at Manoa, Kane'ohe, HI, USA

⁶ Marine Biology Laboratory, Centre for Genomics and Systems Biology, New York University Abu Dhabi, Abu Dhabi, United Arab Emirates

⁷ School of Aquatic and Fishery Sciences and the Burke Museum of Natural History and Culture, University of Washington, Seattle, WA, USA

⁸ ARC Centre of Excellence for Coral Reef Studies, James Cook University, Townsville, QLD, Australia

⁹ College of Science and Engineering, James Cook University, Townsville, QLD, Australia

Abstract:

Environmentally mediated transformations of ecological communities can influence ecosystem functioning. Coral reef fishes are hypothesized to be vulnerable to globally rising temperatures, but cascading effects of organismal tolerances on the assembly and functioning of reef fish communities are largely unknown. Here, we show that cryptobenthic reef fish assemblages on the world's hottest reefs in the southern Arabian Gulf have half the species density and less than 25% the individual density compared to the thermally benign nearby Gulf of Oman, despite comparable benthic community composition and live coral cover. Nevertheless, this pattern is not driven by intrinsic organismal temperature tolerances. Rather, impoverished body conditions of populations in the Arabian Gulf point toward an increased energetic costs of growth and homeostasis at higher temperatures, while intraspecific differences in the diversity and composition of ingested prey items between locations suggest that Arabian Gulf populations need to meet these energetic costs with a different and narrower set of prey resources. As such, the prevailing conditions in the southeastern Arabian Gulf may prohibit the persistence of many small-bodied ectotherms and, ultimately, cause the reduced production, transfer, and replenishment of biomass through cryptobenthic fish assemblages. Consequently, future reefs may lose a critical building block of their fast-paced dynamics, independent of live coral loss.

Introduction:

Why do some species occur in a given location while similar taxa are missing? And how do resulting species assemblages affect rates of ecological processes? As escalating

human impacts on the biosphere deplete and re-shuffle biological communities across ecosystems^{1,2}, answers to these questions are key to our quest to preserve biodiversity and ecosystem services to humanity^{3,4}.

A species' presence at a given location is mediated by a hierarchical interplay between organismal traits (e.g., temperature tolerance, trophic niche), environmental conditions (e.g., temperature, salinity), biogeographic history, and stochastic events (e.g., extinction, dispersal, lottery dynamics)^{5–8}. Furthermore, the identity and diversity of species affect rates of ecosystem functioning, including processes that are critical to human well-being, such as primary or consumer productivity^{9–11}. However, by modifying abiotic conditions, species' niches, and biotic interactions, global stressors such as climate change can interfere with these dynamics through numerous pathways^{12–14}. At the organismal level, changes in environmental factors, particularly temperature, affect internal physiological processes in ectotherms¹⁵, which, if not lethal, will alter organismal energy expenditure^{16–18}. Changes in organismal energy demands subsequently drive resource acquisition (e.g. feeding rates, prey species) and how resulting energy is allocated to life-supporting processes (homeostasis), growth, and reproduction^{19–22}. Dynamics of energy acquisition and investment, which are often investigated through the lens of ecological niche and fitness, are the basis of modern coexistence theory and critical for our understanding of community assembly dynamics²³ and the rate of ecological processes that underpin energy and nutrient fluxes through ecosystems²⁴. Integration across levels of biological organization is, therefore, crucial to understand the effects of global environmental change on our planet's ecosystems²⁵.

Coral reefs are the most diverse marine ecosystem, and their productivity provides vital services for more than 500 million people worldwide²⁶. Scleractinian corals, the foundation species of tropical reefs, show high thermal sensitivity that has led to the rapid global decline of coral reef ecosystems²⁷. In wake of losing coral habitat, communities of the most prominent reef consumers, teleost fishes, can decline or shift in composition^{28–31}, which directly affects the provision of resources to people dependent on reef fisheries³². Nevertheless, recent evidence suggests that many fish species will be able to cope with (or even benefit from) live coral loss, at least in the short-term^{32–34}. However, tropical marine ectotherms are typically adapted to a relatively narrow thermal environment, so reef fishes may also be vulnerable to the direct effects of changing water temperatures^{16,35,36}. Consequently, the direct responses of reef fishes to climate change and their potential to adapt to different thermal regimes might be as important as indirect, habitat-mediated responses^{37–39}.

Despite marked differences in species-specific tolerances to higher temperatures^{40–44}, most reef fish species suffer from non-lethal⁴⁵ adverse physiological, developmental, or behavioral responses when exposed to temperatures outside of their normal range. Current understanding suggests long-term deleterious effects on reef fish populations in the wild³⁷, but few cases of direct temperature-mediated population declines have been documented for *in situ* reef fish communities⁴⁶. One factor that ameliorates the adverse effects of rising temperatures in the wild may be transgenerational acclimation and adaptation, which can enhance the performance of offspring in higher temperatures through developmental, genetic, or epigenetic pathways^{39,47}. Transgenerational adaptation has been shown in a few model

species^{39,47,48}, but demands increased energetic investments^{47,49}. It is presently unresolved whether this process can truly enhance the survival of reef fishes in competitive, uncontrolled environments and how species-specific temperature tolerance differences may mediate coexistence in ecological communities.

Cryptobenthic fishes are the smallest of all reef fishes, rarely exceeding 50mm in maximum body size⁵⁰. They account for almost half of all reef fish species and are numerically abundant and ubiquitous on reefs worldwide^{50–53}. Due to their small body size, these fishes have evolved a unique life history strategy of rapid growth, high mortality, and continuous larval replenishment, and they may play an important role in coral reef trophodynamics⁵⁴. Their small body size and associated life-history also promise exceptional traceability concerning the effects of, and responses to, increasing temperatures⁵⁰. Limited gill surface area, unfavorable mass to surface ratios, high mass-specific metabolism, and other physiological challenges resulting from their minute size suggest that cryptobenthics are particularly susceptible to temperature fluctuations^{42,50,55}. Due to their limited mobility and close association with the benthos⁵⁶, mitigation of temperature extremes through migration is often not viable, and notable community composition shifts following changes in the benthic community structure have been detected^{31,57}. However, their extremely high generational turnover (7.4 generations per year in some species^{54,58}) and prevalence of benthic clutch spawning and parental care⁵⁰ may make them ideally suited for transgenerational adaptation to changing conditions³⁷. In fact, an extremely fast evolutionary clock has been implicated as a driver for rapid speciation in cryptobenthic fishes⁵⁹, which may permit similarly fast microevolutionary changes (i.e., rapid adaption). Thus, cryptobenthic fishes may be

well-suited to detect the impact of environmental change on organisms and populations, with promising insights into whether transgenerational plasticity or adaptation can provide pathways to the persistence of coral reef fishes in warming oceans.

Here, we quantify cryptobenthic community structure, species- and population-specific physiological and dietary traits, and contributions to ecosystem functioning in the world's hottest and most extreme coral reef environment, the southeastern Arabian Gulf, and we compare the resulting patterns with the spatially proximate, but more thermally moderate, Gulf of Oman. Specifically, the goal of our study was to 1) describe cryptobenthic fish assemblages across the two locations, 2) identify organismal traits that permit or preclude existence in the Arabian Gulf, and 3) determine the consequences of these results for the production, provision, and renewal of cryptobenthic fish biomass²⁵.

Results:

Temperatures on reefs in the shallow southern Arabian Gulf can range from 16° C in the winter months to over 36° C in the summer, while reefs in the nearby Gulf of Oman fluctuate within a much narrower temperature range (approximately 22° C to 32° C)⁶⁰. Maximum temperatures on reefs along the Arabian Gulf coast of the United Arab Emirates mirror forecasted temperatures for most tropical coral reefs in the end of the century⁶¹. Despite the seemingly unfavorable conditions for tropical reef building corals, corals have persisted in this region for approximately 15,000 years, with the modern coastline harboring coral reef structures for circa 6,000 years⁶¹. Therefore, the Arabian Gulf represents an exceptional natural laboratory to examine the capacity of reef

organisms to cope with unfavorable conditions and how this influences the diversity and dynamics that underpin modern coral reefs (Fig. 1a,b).

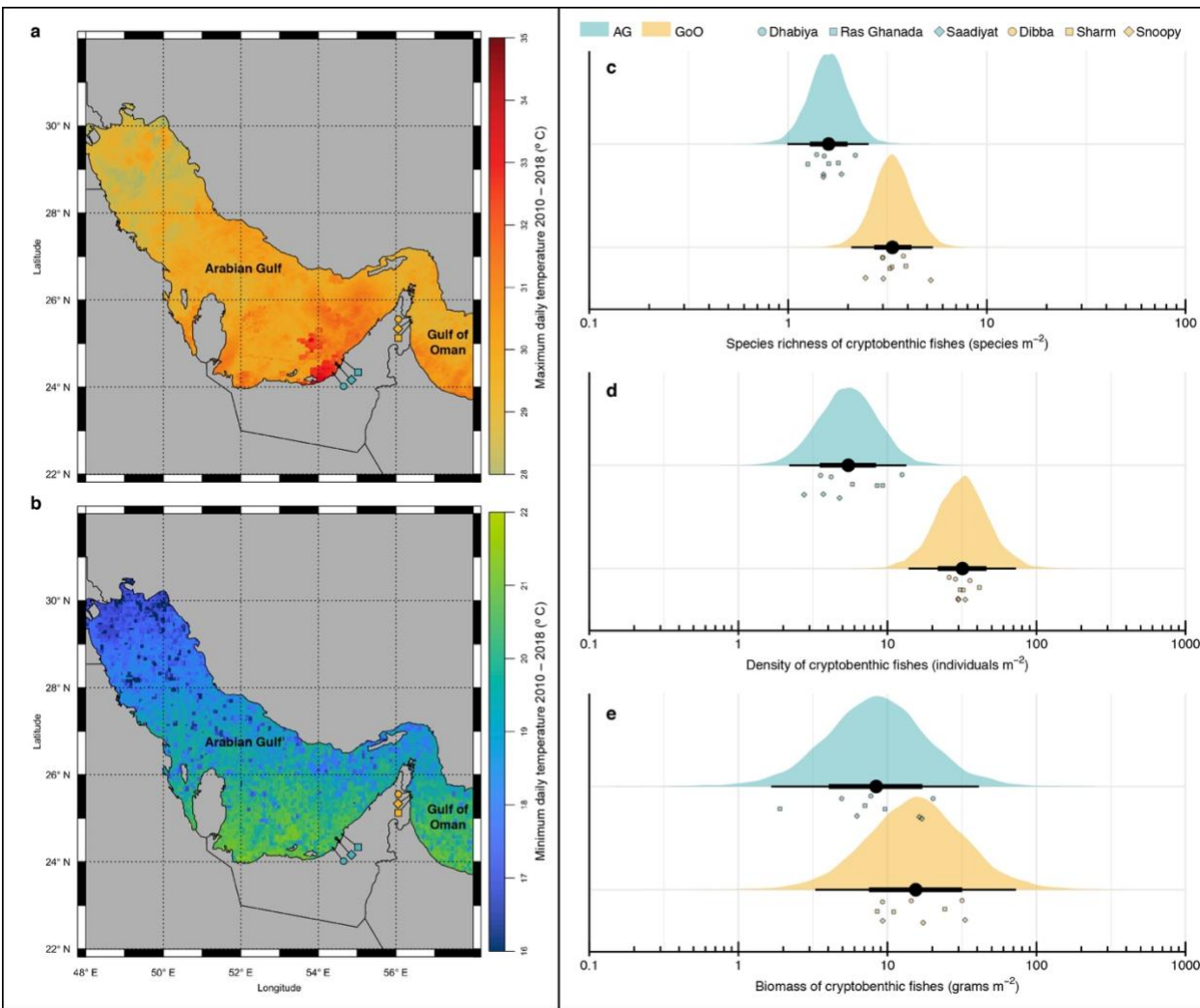


Fig. 1 | Map of the study system and community structure of cryptobenthic reef fish communities in the Arabian Gulf (AG) and Gulf of Oman (GoO). (a–b) Maximum and minimum daily temperature estimates for the AG and GoO between 2010 and 2018 (obtained from MODIS Aqua; <https://oceandata.sci.gsfc.nasa.gov/MODIS-Aqua/Mapped/Daily/4km/sst>), with the study sites indicated. (c) Species density and (d) individual density of cryptobenthic reef fishes was markedly higher on reefs in the GoO, while (e) biomass did not substantially differ between the two locations. Density curves represent predicted values based on 1,000 draws from Bayesian hierarchical linear models testing for differences between locations, while black caterpillar plots represent their means, 50%, and 95% credible intervals. Circles, squares, and diamonds represent raw values from the respective sites in each location, jittered on the y-axis.

Cryptobenthic reef fish assemblages markedly differed between the Arabian Gulf and the Gulf of Oman. Reefs in the Gulf of Oman harbored a higher diversity (Bayesian hierarchical model estimate: *Gulf of Oman*: $\beta = 0.73$ [0.44, 1.01; lower and upper 95% credible interval]) and density (*Gulf of Oman*: $\beta = 1.77$ [1.03, 2.58]) of cryptobenthic fishes (Fig. 1c,d), but standing biomass estimates were comparable (*Gulf of Oman*: $\beta = 0.63$ [-0.54, 1.71]; Fig. 1e). Similarly, the composition of cryptobenthic communities greatly varied between the two locations (Fig. 2a), with no overlap among convex hull polygons in the non-metric multidimensional scaling (nMDS) ordination and a strong effect of *Location* in the PERMANOVA using a site-by-species dissimilarity matrix (*Location*: $df = 1$, $F = 13.58$, $P = 0.001$, $R^2 = 0.46$). There were 29 unique species in the Gulf of Oman, 13 unique species in the Arabian Gulf, and 16 species shared among the two locations. Importantly, of the 29 unique Gulf of Oman species, 89.7% have records from the northern Arabian Gulf in Kuwait and Saudi Arabia (but not the southeastern region), where summer conditions are much less extreme⁶² (Fig 1; Table S1). In contrast to the cryptobenthic fish community, there were no differences in coral cover (Bayesian hierarchical model: *Gulf of Oman*: $\beta = 0.02$ [-1.30, 1.42]) nor overall benthic community structure as revealed by a PERMANOVA (*Location*: $df = 1$, $F = 1.63$, $P = 0.187$, $R^2 = 0.09$; Fig. 2b). Thus, despite broadly comparable benthic conditions, including similar live coral cover, cryptobenthic fish assemblages strongly differed between the two locations.

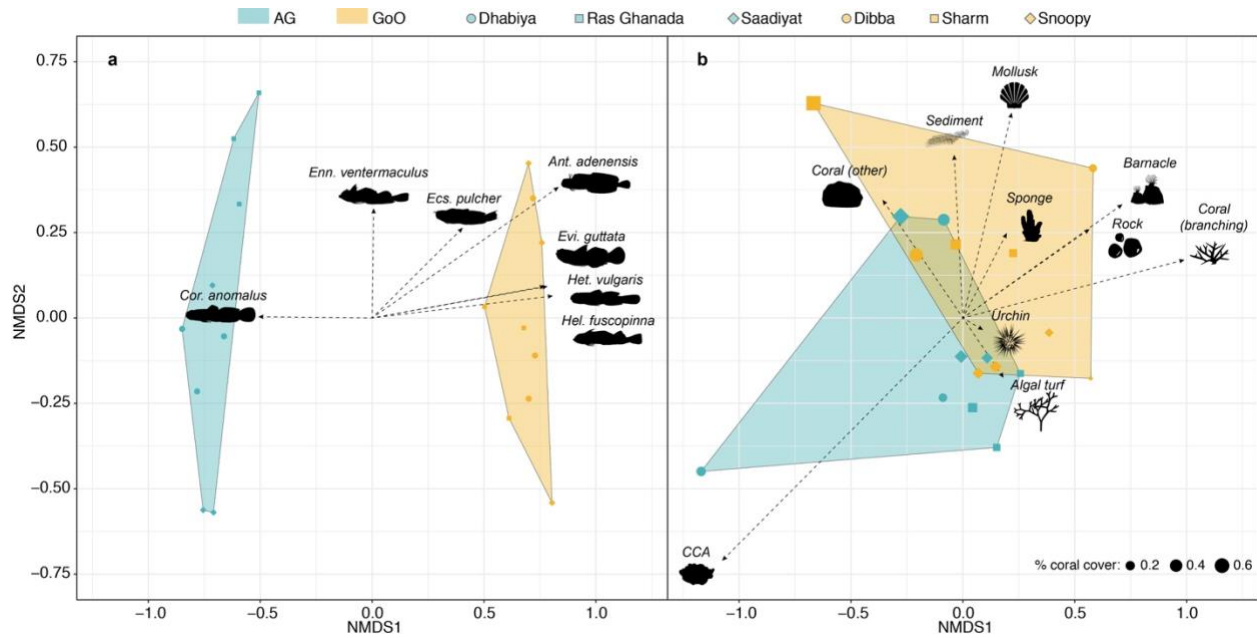


Fig. 2 | Community composition of cryptobenthic reef fishes and benthic functional/taxonomic groups in the Arabian Gulf (AG) and Gulf of Oman (GoO). (a) Biplot of a non-metric multidimensional scaling (nMDS) ordination on cryptobenthic fish communities, with the arrows indicating the position and strength of the seven most important species. (b) Biplot of an nMDS on benthic functional groups, with the influence of all groups indicated with arrows. Convex hull polygons delineate the two locations. Each point represents a sample station at a particular site, with the shape size in (b) scaled by percent live coral cover.

We then tested whether organismal temperature tolerance can explain the absence of species from the thermally extreme southeastern Arabian Gulf, despite their recorded presence in more benign parts of the Arabian Gulf. Notwithstanding distinct thermal regimes at the two locations and the drastic differences in cryptobenthic fish assemblages, species-specific critical thermal tolerance limits did not explain the absence of three common Gulf of Oman species in the Arabian Gulf (Fig. 3). The mean critical thermal maximum tolerance limits (ct_{max}) of all species, regardless of origin, equaled or surpassed the maximum summer temperatures typically recorded in the Arabian Gulf (36.0 °C). *Helcogramma fuscopinna* (a Gulf of Oman species) had the lowest heat tolerance at 36.0 ± 0.11 °C, while *Coryogalops anomalus* from the Arabian

Gulf had the greatest heat tolerance (38.4 ± 0.06 °C). While there were no population differences in heat tolerance for *Enneapterygius ventermaculus* (possibly due to limited samples from the Gulf of Oman), the Arabian Gulf population of *Ecsenius pulcher* showed considerably greater heat tolerance than their Gulf of Oman counterparts, providing evidence for enhanced thermal tolerance in this species. Despite considerable interspecific differences and evidence for intraspecific thermal plasticity (Table S2), mean predicted maximum posterior heat tolerances of all species restricted to the Gulf of Oman were within the 95% bounds of the species present in the Arabian Gulf.

In terms of critical thermal minima (ct_{min}), all species, regardless of origin, tolerated the minimum winter temperature of the UAE Arabian Gulf at 16 °C. Among individuals sampled from the Gulf of Oman population, *E. pulcher* had the greatest tolerance to cold ($ct_{min} = 11.3 \pm 0.1$ °C), while *E. ventermaculus* had the poorest tolerance (13.3 ± 0.1 °C). The cold-tolerance of *E. ventermaculus* in the Arabian Gulf substantially exceeded its Gulf of Oman counterpart (Table S3), which provides evidence from a second population for intraspecific plasticity in thermal tolerances across the two locations. Although there were again species-specific differences in the critical thermal minimum, mean cold tolerances of all Gulf of Oman species also fell within the 95% credible bounds of the species present in the Arabian Gulf (Fig. 3a).

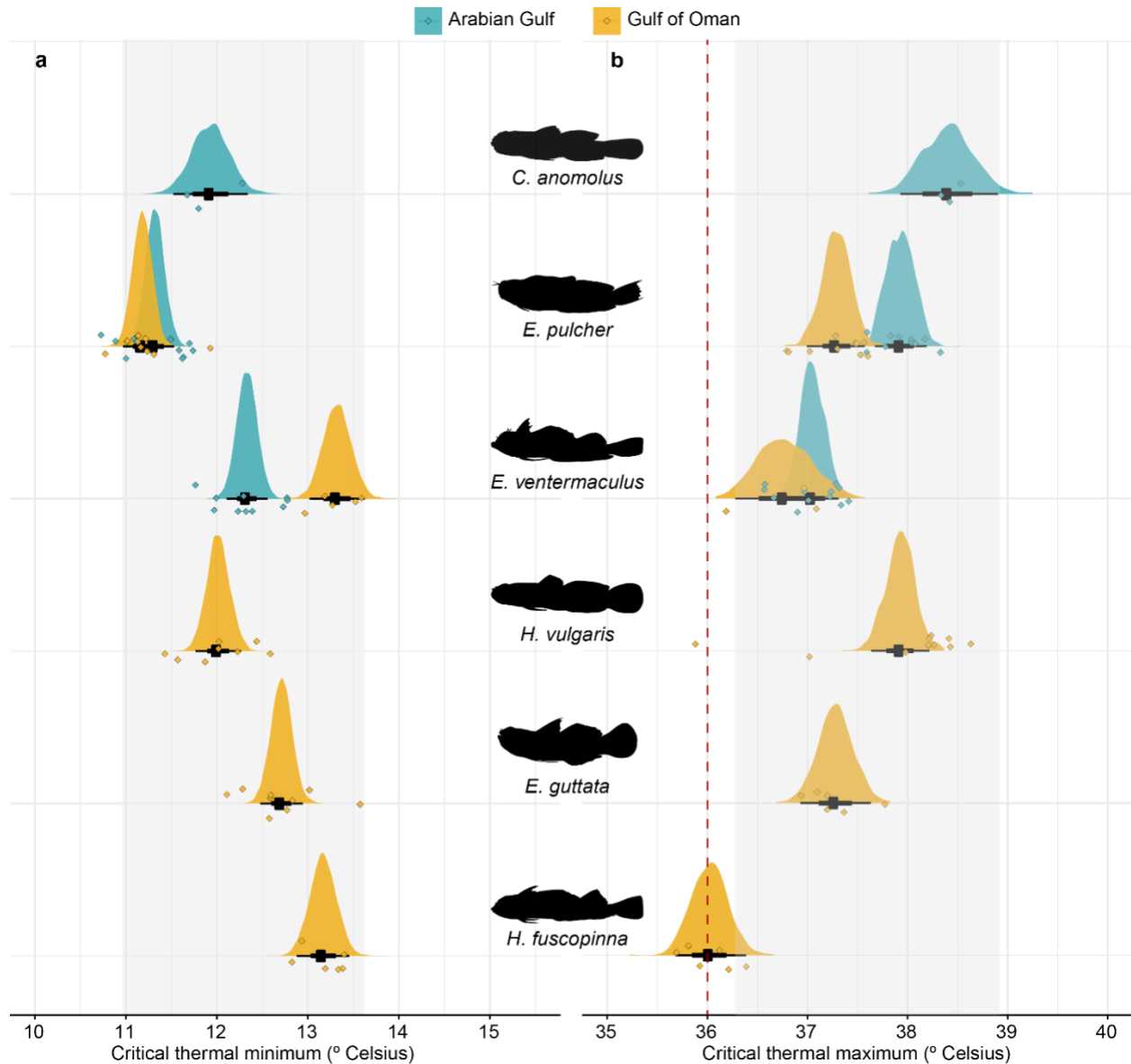


Fig. 3 | Critical thermal tolerance limits of cryptobenthic fish species from the Arabian Gulf and Gulf of Oman. (a) Critical thermal minima ranged between 11.9 °C and 13.3 °C, well below the minimum recorded winter temperature for the southern Arabian Gulf (16.0 °C). (b) Critical thermal maxima ranged between 36.0 °C and 38.4 °C, but they were above or equal to the maximum recorded summer temperature in the Arabian Gulf (36.0 °C; red dashed line). Density curves represent fitted values based on 10,000 draws from Bayesian linear models that test for differences among all populations, while black caterpillar plots represent their means, 50%, and 95% credible intervals. Diamonds represent raw values, jittered on the y-axis. Grey boxes delineate the range of the 95% credible intervals obtained for the three species present in the Arabian Gulf.

To further examine potential drivers of cryptobenthic community structure, we quantified species' prey ingestion in the two locations using gut content DNA

metabarcoding⁶³ across 88 individuals belonging to six species (*C. anomolus*, *E. pulcher*, and *E. ventermaculus* [Arabian Gulf and Gulf of Oman populations]; *Antennablennius adenensis*, *Eviota guttata*, and *Heteroleotris vulgaris* [Gulf of Oman only]). We targeted the cytochrome c oxidase subunit I (COI) gene region with primers that preferentially amplify metazoans and the 23S rRNA gene region with primers designed to amplify algae. Across all examined fishes, COI metabarcoding yielded a total of 547 unique operational taxonomic units (OTUs), while 23S metabarcoding yielded 3,009 unique exact sequence variants (ESVs). Bipartite dietary network trees and modularity analyses for the COI marker showed strong separations between the Arabian Gulf and Gulf of Oman populations (Fig. 4). The COI network contained five distinct modules (modularity = 0.472), with 92.3% of individuals from the Arabian Gulf distributed across two modules. Module V contained seven out of ten individuals of *C. anomolus* from the Arabian Gulf, 8 out of 9 individuals of *E. ventermaculus* from the Arabian Gulf, and one *E. guttata* from the Gulf of Oman. The remaining individuals of *C. anomolus* and *E. ventermaculus* from the Arabian Gulf clustered with *E. pulcher* from the Arabian Gulf (five out of seven), four Gulf of Oman individuals of *C. anomolus*, and a single *H. vulgaris* in module II (Fig. 4a,b). The 23S marker also revealed five modules (modularity = 0.359) but showed an even stronger regional separation. All individuals from the Arabian Gulf (except for one *C. anomolus*) were united in a single module (module III), which contained no Gulf of Oman individuals (Fig. 4c,d). While some species separated into distinct modules, location specific differences superseded taxonomic boundaries. With the exception of *C. anomolus*, species occurring in both

locations showed strong dietary differences, while broadly overlapping with other species in the Gulf of Oman.

Prey diversity rarefaction curves in the Gulf of Oman showed that *E. pulcher*, a purportedly herbivorous species⁶⁴, ingested the widest variety of animal prey species (COI marker), followed by *E. ventermaculus* (Fig. S1). For both species, Gulf of Oman populations consumed a higher diversity of prey items than Arabian Gulf populations. Only *C. anomolus* showed no clear difference in extrapolated values (although diversity was higher for Gulf of Oman populations for the interpolated value). For algal prey items (23S marker), prey diversity was again higher in Gulf of Oman populations of *E. pulcher* and *E. ventermaculus*, while the opposite was evident for *C. anomolus*. Overall, Gulf of Oman populations of *E. ventermaculus* ingested the highest autotroph prey diversity, followed by Arabian Gulf populations of *C. anomolus*.

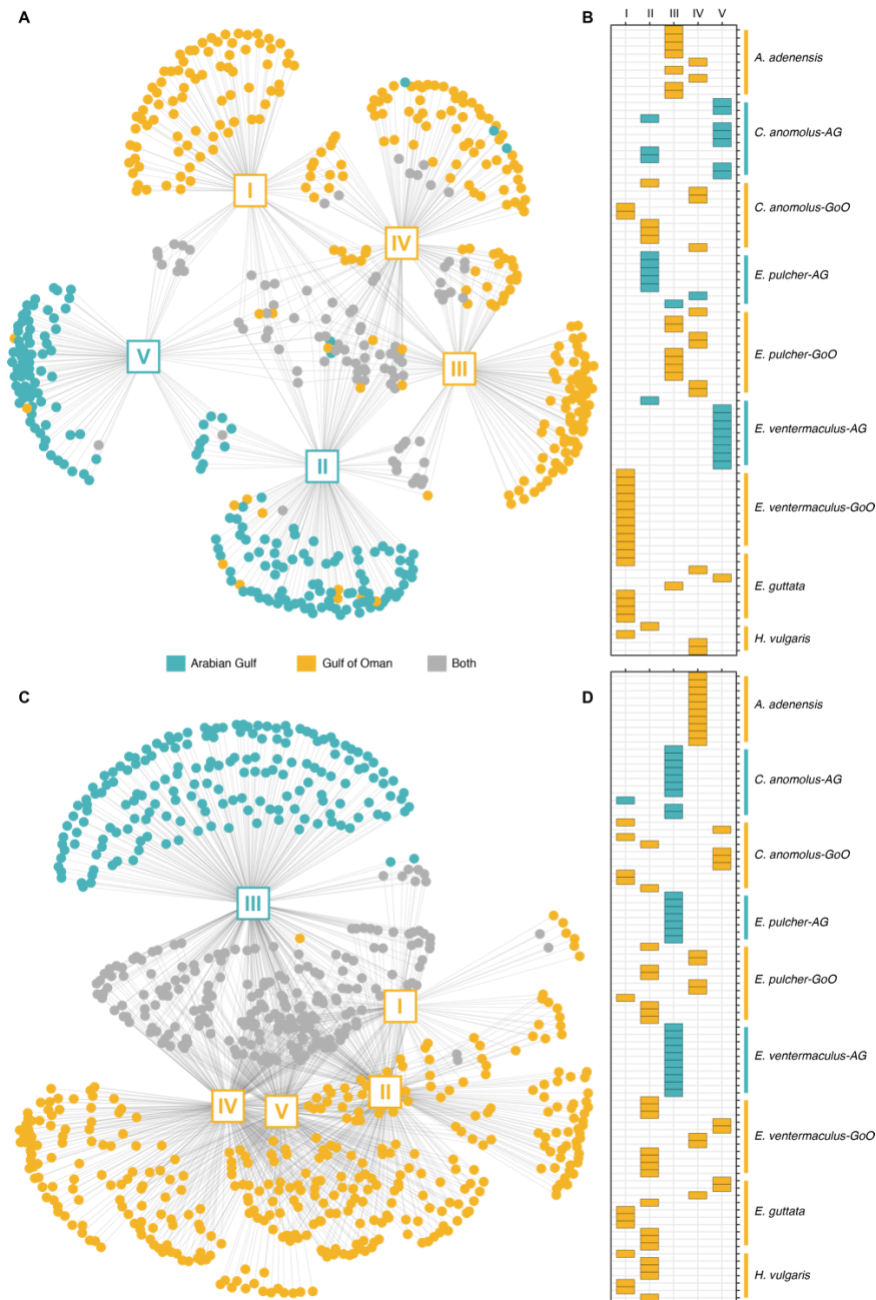


Figure 4 | Diet network trees and modularity mosaics showing differences in ingested prey items and individual-based module membership for COI (a,b) and 23S (c,d) markers. (a,c) Squares with roman numerals represent the recovered modules as nodes in the network tree, while dots represent unique prey items. Blue dots are OTUs (COI) or ESVs (23S) found only in individuals from the Arabian Gulf, gold symbols are from the Gulf of Oman individuals, and grey symbols represent prey items found in individuals from both locations. **(b,d)** Results of the modularity analysis with modules (I-V) as columns and individuals within each species as rows. Colored squares indicate membership in a given module.

272 We further examined the potential organismal and ecosystem-wide energetic
273 consequences of thermal regimes and resource availability between the two locations
274 by first assessing length-weight relationships of three co-occurring species, and then by
275 modeling individual-based growth and mortality to estimate community-wide biomass
276 cycling. We employed Bayesian linear models to test the effects of total length (*TL*) and
277 *Location* on *Weight*, which showed clear effects of *Location* across all species, with Gulf
278 of Oman populations consistently having higher weights for a given body length (*E.*
279 *ventermaculus*: *Gulf of Oman*: $\beta = 0.16$ [0.13, 0.19], *C. anomolus*: *Gulf of Oman*: $\beta =$
280 0.15 [0.09, 0.21], and *E. pulcher*: *Gulf of Oman*: $\beta = 0.19$ [0.14, 0.25]) (Fig. 5). Notably,
281 empirical values for the largest individuals of *C. anomolus* from the Arabian Gulf were
282 consistently below the model fit, suggesting worse body conditions than predicted by
283 the model and substantially worse body conditions than Gulf of Oman individuals of
284 comparable size (Fig 5b). In contrast, no clear differences emerged between the
285 abundances of the three species' populations across locations (effect size uncertainties
286 intersected zero), although *E. ventermaculus* (*Gulf of Oman*: $\beta = 0.89$ [-1.08, 2.86) and
287 *E. pulcher* (*Gulf of Oman*: $\beta = 3.46$ [-0.42, 9.93]) showed a trend toward lower
288 abundances in the Arabian Gulf, while *C. anomolus* exhibited the opposite trend (*Gulf of*
289 *Oman*: $\beta = -0.94$ [-3.82, 1.69]).

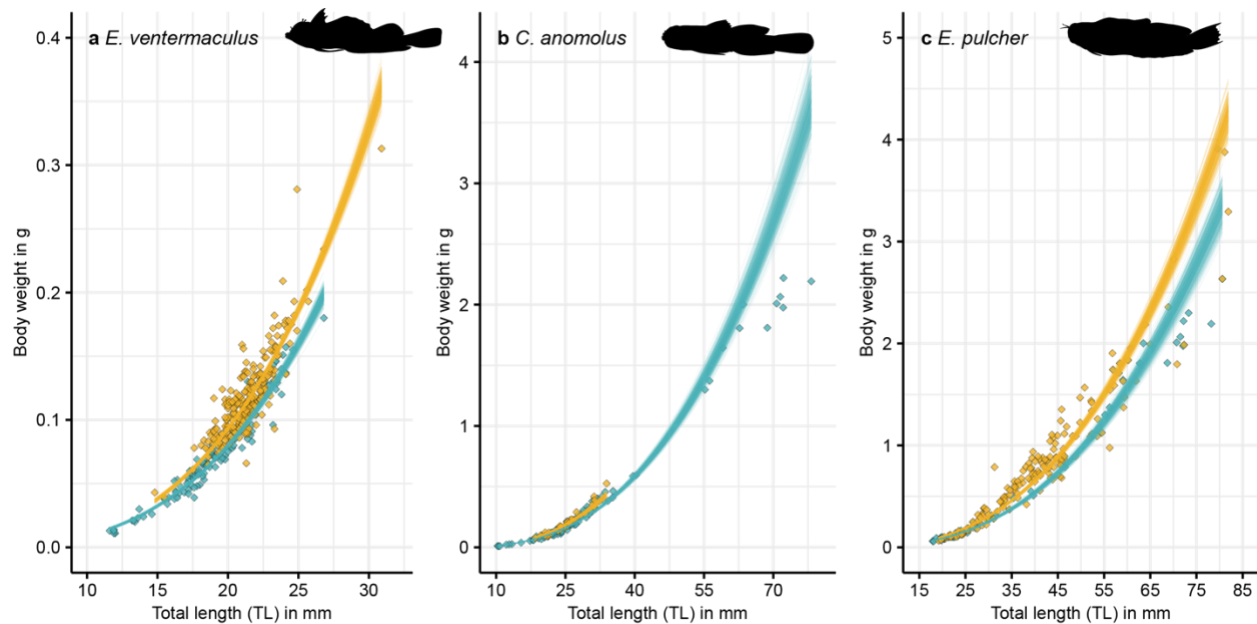


Figure 5 | Relationships between total length (TL) and body weight in populations of *Enneapterygius ventermaculus* (a), *Coryogalops anomolus* (b), and *Ecsenius pulcher* (c) in the Arabian Gulf (blue) and Gulf of Oman (gold). Each line represents a fitted draw from 500 iterations based on the posterior parameters from a Bayesian model regressing length against weight (thus showing model fit uncertainty). Diamonds represent raw values for individual fishes.

Finally, modeling individual-based growth and mortality for cryptobenthic fish communities at each site revealed strong differences in the ecological dynamics that underpin ecosystem functioning between the Arabian Gulf and Gulf of Oman (Fig. 6). Biomass production was almost one order of magnitude higher on reefs in the Gulf of Oman (0.231 ± 0.025 [mean \pm SE] $\text{g d}^{-1} \text{m}^{-2}$) compared to the Arabian Gulf ($0.038 \pm 0.014 \text{ g d}^{-1} \text{m}^{-2}$), while consumed biomass was more than five times higher (0.039 ± 0.015 vs. $0.007 \pm 0.001 \text{ g d}^{-1} \text{m}^{-2}$). Turnover was also higher in the Gulf of Oman ($0.017 \pm 0.005 \text{ \% d}^{-1}$) compared to the Arabian Gulf ($0.006 \pm 0.005 \text{ \% d}^{-1}$). Therefore, reefs in the two locations exhibit contrasting productivity dynamics at various levels of organization. In the Arabian Gulf, individual fishes accumulate less body mass per

millimeter of body length and collectively, cryptobenthic communities produce, provide, and replenish consumer biomass at much lower rates than Gulf of Oman communities.

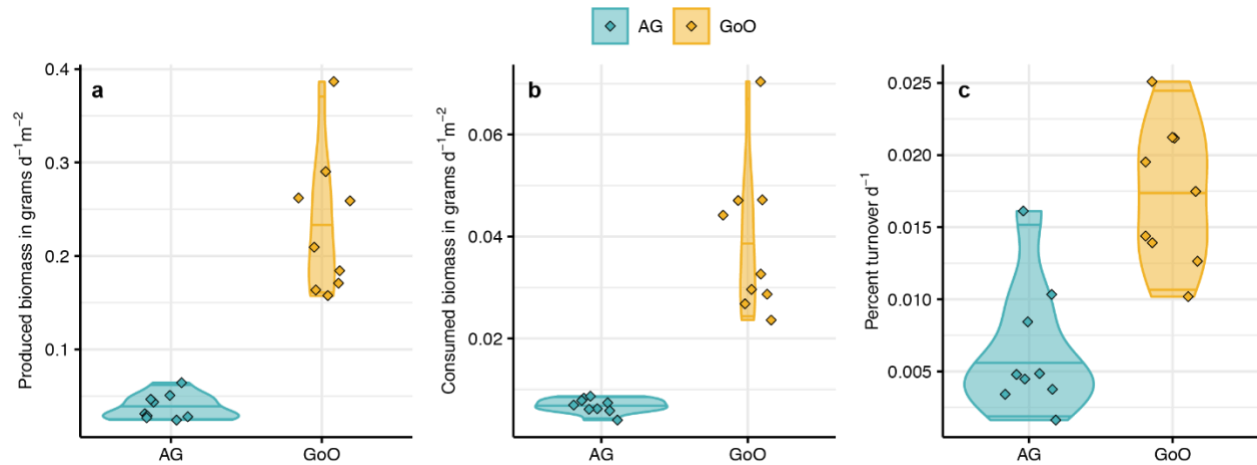


Figure 6 | Model estimated biomass production, consumption, and turnover in cryptobenthic fish assemblages across the two locations. (a) Produced biomass (grams of fish tissue grown per day and m^2). **(b)** Consumed biomass (grams of fish tissue perished per day and m^2). **(c)** Percent turnover (renewal of produced and consumed biomass per day). Violin plots and lines represent medians and variance estimates (95% quartiles) for the three metrics across the two locations. Diamonds represent values for each sampled cryptobenthic reef fish community across the six sites (three per site).

Discussion:

As rapid environmental change sweeps across the Earth's ecosystems, understanding the processes that underpin local community structure and ecosystem functioning is urgent. Here, we show that cryptobenthic fishes on the world's hottest reefs in the southeastern Arabian Gulf have reduced diversity, abundance, and body condition compared to reefs with more moderate temperatures in the nearby Gulf of Oman, despite similarities in live coral cover and benthic community structure. While species with populations in both locations exhibit shifted tolerances to thermal extremes that may enable survival in Arabian Gulf conditions, species-specific temperature tolerances

are not the main driver of species presence/absence in the Arabian Gulf. Rather, poor body condition in Arabian Gulf populations suggest that physiological responses to Arabian Gulf conditions (related to temperature and possibly other environmental variables) might invoke energetic costs that can only be borne by species with low metabolic demands. Furthermore, intraspecific differences in the diversity and composition of prey indicate that cryptobenthic fishes in the Arabian Gulf need to meet these increased costs with a distinct and restricted suite of prey items. These individual energetic challenges have far reaching consequences for ecosystem-scale energy and nutrient fluxes; even conservative estimates of cryptobenthic reef fish productivity in the Arabian Gulf are an order of magnitude lower than the Gulf of Oman. Our results indicate that cryptobenthic reef fish assemblages on future coral reefs may be shaped by species-specific individual energy deficits that decrease the rate of biomass production, transfer, and renewal through small vertebrate consumers, thereby eroding a cardinal component of heterotrophic coral reef productivity⁵⁴.

Organismal responses

As the smallest and shortest-lived marine vertebrates, responses of cryptobenthic fishes to extreme temperatures should be easy to trace⁵⁰. Yet, critical thermal tolerances of all tested species from both locations were equal to or greater than the extreme maximum summer temperatures of the southeastern Arabian Gulf^{43,45,65}. The high intrinsic tolerance of species from the thermally moderate Gulf of Oman aligns with previous results of high, short-term critical thermal tolerances in cryptobenthics⁴³. Furthermore, swift generational turnover in cryptobenthic fishes could facilitate transgenerational

thermal plasticity and increased thermal tolerance^{54,58}. Collectively, this should have permitted their colonization and persistence in the geologically young southeastern Arabian Gulf⁶⁶, since no hard biogeographic boundary exists between the Gulf of Oman in the Arabian Gulf⁶⁰. Indeed, 26 out of 29 (89.7%) cryptobenthic fish species from the Gulf of Oman that were absent from the southeastern Arabian Gulf (where temperatures are highest in the summer, but moderate in the winter) have been recorded in the cooler Arabian Gulf regions of Saudi Arabia and Kuwait (Table S1)^{62,67,68}. Thus, neither thermal tolerances to short-term temperature extremes nor biogeographic history are likely to drive the observed depauperate cryptobenthic communities on Earth's hottest coral reefs.

Instead, temperature-driven demands on an individual's energetic budget and the inability of small-bodied fishes to meet these demands may mediate existence on these extreme reefs. Transgenerational acclimation or adaptation of fishes to increasing temperatures comes with substantial energetic costs^{39,47,69} that are reflected in reduced body condition^{22,70,71}. Such costs (driven by either extremely high temperatures or overall thermal variability) are evident in the lower mass per unit body length of Arabian Gulf populations in the three examined species. Although shifts in transgenerational temperature tolerance may permit survival and adequate performance in controlled laboratory conditions^{39,47}, our results show that acclimation to warmer water and its associated energetic costs may not be viable for most cryptobenthics in natural environments where they continuously engage in costly activities such as foraging and escaping predators⁷⁰.

In the southeastern Arabian Gulf, this energetic challenge may be further exacerbated by fundamentally different prey resources and reduced prey diversity; indeed, gut content metabarcoding revealed a different and narrower range of both primary and secondary prey resources ingested by individuals from the Arabian Gulf. Shifts in prey composition can require changes in digestive morphology and processes that further alter species' energy budgets^{72,73}, while a lower diversity of prey items can reduce individual and population persistence^{74,75}. Naturally, energetic challenges would be even greater if prey in the Arabian Gulf has less favorable nutritional profiles or energy densities⁷⁶. While we did not investigate differences in diet quality (i.e., nutrient content) across locations, large reef fish species in the Arabian Gulf have been shown to ingest unusual diets dominated by nutritiously poor benthic invertebrates⁷⁷.

Moreover, the goby *Coryogalops anomolus* was the only cryptobenthic species to show weakly distinct prey composition between locations and higher autotroph prey richness in the Arabian Gulf, and it was also the only species with a higher abundance and larger body size in the Arabian Gulf as compared to the Gulf of Oman. This species also had a less pronounced reduction in body condition from the Gulf of Oman to the Arabian Gulf compared to *E. pulcher* and *E. ventermaculus*. As opposed to most dominant cryptobenthic genera in the Arabian Gulf and Gulf of Oman (e.g. *Ecsenius*, *Eviota*, *Enneapterygius*, etc.), the goby genus *Coryogalops* belongs to a clade that contains many non-reef associated species from comparatively extreme habitats^{78,79}. For example, *Coryogalops* often inhabit tidepools and other shallow environments exposed to fluctuating temperatures and salinity where they rely on a sedentary lifestyle with low energetic costs^{80,81}. Thus, the persistence of *C. anomolus* in the southeastern

Arabian Gulf may reflect an adaptation to extreme environments afforded by its evolutionary history of belonging to a lineage of non-reef, extreme habitat specialists.

Our results indicate that species-specific capacities to cope with the energetic costs of inhabiting extreme environments, rather than the direct effects of temperature *per se* or its effect on benthic community structure (cf.⁶⁵), underpin the reduced diversity and abundance of cryptobenthic fishes on these extreme reefs. For cryptobenthics, which already exhibit high energetic demands per gram of body mass and rapid growth⁵⁰, increased cost of growth and homeostasis appear to represent a significant challenge. Along with environmentally-driven differences in prey composition and diversity (as well as potential reductions in nutritional value or energetic densities), this may create an energetic double jeopardy that represents an insurmountable obstacle for many cryptobenthic species. Further decreases in body size (a universal physiological response to warmer temperatures^{18,22}) might simply not be possible for many cryptobenthic reef fishes that are already at or near the physical minimum body size for vertebrates^{50,55,82}. Therefore, our findings suggest severe consequences of climate change on organismal performance^{83,84}, including their ramifications for species persistence and community assembly⁸⁵, from highly-vulnerable, tropical ectotherms in a natural setting.

Ecosystem-scale consequences

The organismal responses that appear to govern community assembly in the southeastern Arabian Gulf create a sobering perspective on coral reef ecosystem functioning in a warming, more thermally extreme ocean. Coral reefs are some of the

most productive marine ecosystems⁸⁶ that are sustained through a variety of energetic pathways^{87–90}. Among these pathways, benthic productivity⁹¹ and its assimilation and transfer through cryptobenthic reef fishes represents an important bottom-up flux of energy and nutrients to higher trophic levels⁵⁴. The differences in biomass production, transfer, and turnover between cryptobenthic fish communities in the Arabian Gulf and Gulf of Oman suggest that the role of cryptobenthics as vectors of energy and nutrients to larger consumers may be stymied in hot waters. In fact, yearly productivity estimates for cryptobenthic fishes in the Arabian Gulf may be even lower than our model suggests due to the decreased individual-level production of body mass per unit body size and the influence of seasonality effects on growth. Both winter and summer temperatures in the southeastern Arabian Gulf are unfavorable for growth and effectively interrupt the growing season of cryptobenthic fishes (which are predominantly annual species), much as they do with fishes from other seasonal ecosystems⁹². Yet, neither environmental limits on the growing season, nor decreased individual mass per unit body size were considered in the model, which held temperature constant at the mean annual temperature to allow constant growth throughout the year and used constant length-weight coefficients for both locations. Inclusion of these factors would almost certainly further reduce productivity estimates for the Arabian Gulf reefs.

The Gulf of Oman reefs included in this study may be particularly productive environments due to seasonal upwelling⁹³, and indeed, our estimates of cryptobenthic productivity exceeded estimates for a degraded but species-rich reef on the Australian Great Barrier Reef (GBR) (2.31 vs. 0.64 kg ha⁻¹d⁻¹)⁹⁴. In contrast, even the optimistic estimate of 0.38 g ha⁻¹d⁻¹ for the Arabian Gulf compared poorly with the same degraded

GBR-reef. Notably, the study site on the GBR had undergone a sequence of severe disturbances⁹⁴, which greatly reduced space and shelter availability for small-bodied fishes; yet, it retained a diverse assemblage of cryptobenthic fish species that were likely able to satisfy their energetic demands due to benign temperature profiles³⁰. At the time of our survey, reefs in the Arabian Gulf had undergone extensive bleaching in previous years^{95–98}, which may have negatively affected the diversity and abundance of cryptobenthic fishes compared to the less disturbed reefs in the Gulf of Oman^{28,99,100}. However, the lack of difference in benthic community structure observed between regions suggests that benthic structure was not a primary driver of the observed patterns. Although the loss of some specialist cryptobenthic species has been reported after substantial live coral cover loss^{95,101}, previous studies have not detected substantial short-term changes in either small reef fish richness and abundance or in overarching ecosystem productivity^{31,33,57,95}.

Our results showcase an imminent threat to cryptobenthic reef fishes and their critical role for coral reef functioning: similar to corals, which are highly susceptible to extreme temperatures²⁷, many of the world's smallest marine ectotherms may struggle to compensate for increasing growth costs as they adapt to warming temperatures. As a consequence, small consumer productivity, energy transfer, and replenishment of biomass at the bottom of the fish food chain may decrease under climate change¹⁸. Analogous to cryptobenthics, the Arabian Gulf harbors less diverse and abundant communities of large reef fishes compared to nearby locations with more moderate temperatures^{102,103}. It remains unresolved whether these patterns are driven by similar mechanisms as proposed herein (e.g., an energetic filtering effect on large fish species)

or relate to decreased productivity at lower trophic levels. Yet, in light of the hypothesized importance of small vertebrate consumers in global food webs¹⁰⁴ and the unique ecological role of cryptobenthics in coral reef trophic dynamics⁵⁴, the effects of elevated temperature on cryptobenthic fish assemblages may considerably reduce ecosystem functioning on future coral reefs.

Methods:

Field sampling

We studied cryptobenthic fish communities in two locations that dramatically differ in their annual temperature profiles. Temperatures in the Arabian Gulf (Dhabiya: 24.36383°, 54.10121°; Ras Ghanada: 24.84743°, 54.69235°; Saadiyat: 24.65771°, 54.48691°) are extremely hot, with summer maximum temperatures reaching up to or above 36 °C, while winter minimum temperatures fall to 16 °C. In contrast, temperatures in the Gulf of Oman (Dibba Rock: 25.55378°, 56.35694°; Sharm Rock: 25.48229°, 56.36695°; Snoopy Rock: 25.49210°, 56.36401°) lie within more typical coral reef temperature profiles throughout the year, ranging from 32 °C to 22 °C (Price et al. 1993). Notably, the sampled reefs in the Arabian Gulf are at the extreme end of high maximum summer temperatures, while being relatively benign concerning the low winter temperatures in the rest Arabian Gulf (Fig. 1a,b).

In April and May of 2018, we sampled six reefs (hereafter *site*) in the southeastern Arabian Gulf and northwestern Gulf of Oman (three sites per location). At each site, we sampled three distinct reef outcrops for cryptobenthic reef fishes using enclosed clove oil stations (Ackerman and Bellwood 2000; Brandl et al. 2017), covering

489 an average of 4.63 ± 0.38 and 4.73 ± 0.16 m² in the Arabian Gulf and Gulf of Oman,
490 respectively, for a total of 18 community samples. Since our sampling was not
491 replicated temporally, we cannot exclude the possibility of annual changes in
492 cryptobenthic communities in the Arabian Gulf. Nevertheless, the lack of records for
493 many of the species found in the Gulf of Oman in the southeastern Arabian Gulf
494 indicates that the depauperate nature of cryptobenthic assemblages in this region is not
495 a function of our sampling at a single point in time. For each station, we covered a reef
496 outcrop with a fine-mesh, bell-shaped net (2.74 m in diameter), weighted by a chain on
497 the bottom. We then covered the same area with an impermeable bell-shaped tarpaulin,
498 also weighted by a chain on the bottom. Then, three to four divers inoculated the area
499 under the net with two liters of clove-oil:ethanol solution (1:5) using collapsible spray
500 bottles (clove bud oil: Jedwards International, Inc., Braintree, MA, USA). Upon emptying
501 the entire solution and a short wait period to allow the clove oil to disperse and take
502 effect (approximately 2-3 mins), we removed the tarpaulin and gently peeled back the
503 net while collecting all fishes found within the inoculated area with tweezers. We
504 searched the entire area, including inside caves and crevices until five minutes passed
505 without a single diver collecting any additional fishes. We placed all fishes into Ziplock
506 bags, brought them to the surface, euthanized them with a clove-oil overdose, and
507 immediately placed them into an ice-water slurry until processing and preservation. At
508 the end of each day, all specimens were brought to the laboratory at NYUAD or the
509 Radisson Blu hotel in Fujairah. To quantify benthic community structure, we used a
510 haphazardly placed 20×20cm PVC-quadrat to frame and take five photographs of the
511 benthos at each sampled outcrop.

In addition to the quantitative samples obtained from the clove-oil stations, we collected cryptobenthic fish individuals for thermal tolerance trials using roving diver collections. Specifically, two divers, each equipped with spray bottles of clove-oil:ethanol solution, a dipnet, and Ziplock bags, searched the reef for cryptobenthic fishes across three species in the Arabian Gulf (*Coryogalops anomolus*, *Ecsenius pulcher*, and *Enneapterygius ventermaculus*) and six species in the Gulf of Oman (*C. anomolus*, *E. pulcher*, and *E. ventermaculus* plus *Eviota guttata*, *Helcogramma fuscopinna*, and *Heteroleotris vulgaris*). Upon locating an individual or identifying a suitable microhabitat in which a fish was suspected, the diver applied the clove-oil solution until the fish showed signs of anesthesia. At the earliest opportunity, we caught the fish with a dipnet and placed it into a ziplock bag. Upon completion of the dive, all fishes were placed in small holding tanks equipped with air stones and periodically replenished with fresh seawater. Upon completion of all collections, fishes were brought to the seawater laboratory facilities at NYUAD. All roving diver collections were performed at Dhabiya Reef (Arabian Gulf) and Snoopy Rock (Gulf of Oman).

Laboratory processing

For samples obtained from the enclosed clove-oil stations, we followed an established protocol that involved photographing, identifying, recording, measuring, weighing and preserving each specimen⁵¹. To photograph the fishes, we placed each individual in a small photo tank and used a Nikon D300 DSLR camera with an AF-S Micro Nikkor 60mm macro lens (f/2.8G ED; Nikon Inc., Melville, NY, USA) against a black or white background. We measured each individual to the nearest 0.1mm using digital calipers

and weighed the individual (wet weight) to the nearest 0.001 grams on a precision jewelry scale. We preserved all individuals in 95% ethanol, either separately or in lots with conspecifics. A subset of the samples was shipped to the University of Washington Fish Collection, where they were cataloged, while the rest were retained and archived at NYUAD.

Benthic photo analysis

For the benthic photographs, we created a grid with 16 equally spaced points which we superimposed on every photograph. We then categorized the benthos at each of the points into functional groups, including barnacles, bleached corals, crustose coralline algae, dead coral, hydroids, branching, encrusting, foliose, and massive live coral, mollusks, bare rock, soft sediment, sponges, algal turf, and sea urchins. Whenever visual identification was not possible (due to obstruction, shading, or blurriness), we categorized the point as “unidentifiable” (n = 69 out of 1,440). All photographs with the grid superimposed will be made accessible with the raw data of the paper.

Critical thermal maximum and minimum trials

We examined individual temperature tolerances by using critical thermal maximum (CT_{max}) and minimum (CT_{min}) trials¹⁰⁶. We transported all fishes caught during roving diver collections to the wet laboratory facilities at NYUAD and housed them for at least 48 hours in large holding tanks. Trials took place from the 9th to 13th of May of 2018. For the trials, a haphazardly selected subset of individuals was moved from the holding tanks into separate chambers filled with seawater at ambient temperature and salinity.

558 Then, after providing individuals with a 15-minute settlement period, we incrementally
559 decreased (CT_{min}) or increased (CT_{max}) the water temperature within the chambers
560 while keeping all other parameters constant. Specifically, we lowered or increased the
561 temperature by 0.1° C every minute¹⁰⁶ while keeping all fishes under constant
562 observation. Critical endpoints were classified as loss of equilibrium or uncontrolled
563 swimming without a righting response for two seconds or more¹⁰⁶. When individuals
564 reached their critical endpoints, they were immediately removed, euthanized with a
565 clove-oil overdose, measured, weighed, and photographed. In total, we processed 60
566 individuals across six species for CT_{max} trials, and 62 individuals across the same
567 species for CT_{min} trials.

568

569 *Gut content DNA metabarcoding*

570 We processed a subset of individuals across six species (*A. adenensis*, *C. anomolus*, *E.*
571 *pulcher*, *E. guttata*, *E. ventermaculus*, and *H. vulgaris*) for gut content DNA
572 metabarcoding at the University of Washington. We haphazardly selected ten, ten, and
573 seven (due to limited sample availability) individuals of *C. anomolus*, *E. ventermaculus*,
574 and *E. pulcher*, respectively, from the Arabian Gulf, and ten individuals each (with the
575 exception of *E. pulcher*, for which we selected eleven individuals) of *C. anomolus*, *E.*
576 *ventermaculus*, *A. adenensis*, *E. guttata*, and *H. vulgaris* from the Gulf of Oman. Then,
577 under sterile conditions, we dissected out the entire alimentary tract and removed all
578 other organs (e.g. liver, gonads) under a Zeiss V20 SteREO dissecting microscope
579 using micro-surgery tools. We placed the entire gut into an extraction tube and

performed DNA extractions with a DNeasy PowerSoil Pro DNA Isolation Kit (Qiagen, Hilden, Germany). We stored all DNA extracts at 4° C until further processing.

All DNA samples were sent to Jonah Ventures (Boulder, Colorado, USA) for two-step PCRs, library preparation, and sequencing. We targeted two universal gene regions: the mitochondrial cytochrome c oxidase subunit I (COI) for metabarcoding metazoan biodiversity and the chloroplast 23S rRNA for metabarcoding algae. For the COI gene, we selected the m1COIintF forward primer¹⁰⁷ and jgHCO2198 reverse primer¹⁰⁸. For the 23S gene, we selected the p23SrV_f1 and Diam23Sr1 23S primers^{109–111}. All COI and 23S primers contained a 5' adaptor sequence to facilitate indexing and sequencing. The PCR reactions for both COI and 23S genes were run at a volume of 25 µl according to the Promega PCR Master Mix guidelines (Promega, Madison, Wisconsin, USA): 12.5 µl Master Mix, 0.5 µM of each primer, 1 µl gDNA, and 10.5 µl DNase/Rnase-free water. For COI, PCR amplification was run with the following conditions: initial denaturation at 94 °C for 2 minutes, followed by 45 cycles of 15 seconds at 94 °C, 30 seconds at 50 °C, and 1 minute at 72 °C, then a final elongation at 72 °C for 10 minutes. For 23S, DNA was PCR-amplified under the following conditions: initial denaturation at 94 °C for 3 minutes, followed by 40 cycles of 30 seconds at 94 °C, 45 seconds at 55 °C, and 1 minute at 72 °C, then a final elongation at 72 °C for 10 minutes. After PCR amplification, each reaction was visually inspected with a 2% agarose gel to ensure successful amplification and determine amplicon size.

All remaining library preparation and sequencing protocols apply to both the COI and 23S markers. Clean-ups were performed by incubating amplicons with Exo1/SAP for 30 minutes at 37 °C, followed by inactivation at 95 °C for 5 minutes, then the

products were stored at -20 °C. Next, a second indexing PCR was performed to bind a unique 12-nucleotide index sequence. The PCR reaction included Promega Master mix, 0.5 µM of each primer, and 2 µl of template DNA. The PCR was performed with the following conditions: initial denaturation at 95 °C for 3 minutes, followed by 8 cycles of 95 °C for 30 seconds, 55 °C for 30 seconds, and 72 °C for 30 seconds. Each reaction was visually inspected with a 2% agarose gel to ensure successful amplification.

25 µl of each indexed amplicon was cleaned and normalized with the SequalPrep Normalization Kit (Life Technologies, Carlsbad, California, USA) according to the manufacturer's protocol. For sample pooling, 5 µl of each sample was added together. Finally, library pools were sent to the Genohub service provider (Austin, Texas, USA). Prior to sequencing, quality control measures were performed, including bead cleaning with Agencourt AMPure XP beads (Beckman Coulter, Brea, California, USA) to remove <200 bp amplicons, sample quantification with a Qubit Fluorometer (Invitrogen, Carlsbad, California, USA), and amplicon average size analysis with an Agilent TapeStation 4200 (Agilent, Santa Clara, California, USA). Finally, sequencing was performed on an Illumina HiSeq using the HiSeq Rapid SBS Kit v2, 500-cycles (Illumina, San Diego, California, USA).

Sequence bioinformatics

For the COI sequences, a joint QIIME¹¹² and UPARSE¹¹³ pipeline was employed for bioinformatic processing. Sequences were demultiplexed and initial quality filtering was performed with QIIME v1.9.1. Primer sequences were trimmed with Cutadapt v1.18¹¹⁴, then forward and reverse reads were pair-end merged with USEARCH

v11.0.667¹¹⁵. Quality filtering was then performed in accordance with the UPARSE pipeline. Sequences were clustered into operational taxonomic units (OTUs) at 99% similarity, and the OTU table was generated by mapping quality-filtered reads back to the OTU seeds. Taxonomy was assigned to OTUs by recording the top basic local alignment search tool (BLASTn¹¹⁶) hit when query coverage and percent identity exceeded 95% and 80%, respectively. GenBank was used as the reference database. When OTU taxonomic assignments did not meet these criteria, taxonomy was removed and recorded as “NA.” Finally, we removed all self-hits from the OTU-dataset, which we identified by matching the highest sequence reads of each species to its individuals, as well as unambiguous (>97% identity match) assignments to species not found in the geographic region (specifically *Oncorhynchus nerka*).

For the 23S sequences, raw sequences were processed with the JAMP pipeline (<https://github.com/VascoElbrecht/JAMP>). After demultiplexing, forward and reverse reads were pair-end merged with USEARCH v11.0.667¹¹⁵. Primers were trimmed from both ends using Cutadapt v1.18¹¹⁴, and quality filtering was conducted with expected error filtering, as implemented through USEARCH¹¹⁷. Reads affected by sequencing and PCR error were removed using the UNOISE algorithm¹¹⁸. Exact sequence variants (ESVs) were then compiled into an ESV table, which included read counts for each sample. Taxonomy was assigned to each ESV by mapping them against a 23S database from Silva¹¹⁹, specifying zero deviations to ensure mapping accuracy. Consensus taxonomy was generated from the hit tables, first considering 100% matches, then decreasing by 1% until hits were available for each ESV. Taxonomy that was present in at least 90% of the hits was reported; otherwise, an “NA” was assigned

when several different taxa matched the ESV. For error reduction due to misidentified taxa, the bracket was increased to 2% when matches of 97% and higher were present, but no family-level or lower taxonomy was assigned.

Data analyses and modeling

To analyze the community variables, we first calculated the surface area (SA) for each sampled outcrop from the curved surface length (CSL) by deriving the sampled outcrop's radius r ($r = 2 \cdot \text{CSL} / 2\pi$), then computing available surface area under the assumption that outcrops are hemispherical constructs ($SA = 4\pi r^2 / 2$). We calculated the sum of individuals, species, and their respective body weight for each station to obtain abundance, diversity, and biomass estimates, which we converted to density estimates by dividing them by the sampled surface area. Using these estimates, we performed three Bayesian hierarchical models, each on the natural logarithm of the response variables (species density, individual density, and biomass per m²). Models were specified to include the fixed effect of *Location* (*Arabian Gulf* vs. *Gulf of Oman*) and the random effect of *Site* (*Dhabiya*, *Ras Ghanada*, *Saadiyat*, *Dibba Rock*, *Sharm Rock*, *Snoopy Rock*) and were run with a Gaussian error distribution. For each model, we ran four chains with 4,000 post burn-in samples, and we validated chain convergence visually. We used the default, non-informative priors set by the *brm* function in the *brms* R package¹²⁰. Then, we used the model parameters to predict distributions based on 1,000 draws from the posterior and plotted the distributions, their mean and confidence bands, and the raw data for each site to evaluate model fit.

671 To examine cryptobenthic fish community composition across the two locations,
672 we created a species-by-sample matrix indicating the abundance of each species in a
673 given sample. We then performed a non-metric multidimensional scaling (nMDS)
674 ordination with the Bray-Curtis dissimilarity matrix of the data in two dimensions (stress
675 = 0.101). We performed a permutational analysis of variance (PERMANOVA) on the
676 same distance matrix (using 999 permutations) and extracted the most influential
677 species using the similarity of percentages (SIMPER) routine. We constructed convex
678 hull polygons for the two locations (as determined by the location of each sample) and
679 plotted them in a biplot with the seven most influential species (average contribution >
680 0.025) superimposed. For benthic community composition, we followed a similar
681 process. After our initial categorization, we first combined live coral categories into
682 “branching” and “other” and omitted all categories with fewer than three records
683 (bleached coral and hydroids) from the data. We also excluded the “unidentifiable”
684 category (<5% of points). We then calculated the proportional contribution of each
685 category to the benthos in a given sampled outcrop and arranged the data into a
686 sample-by-category matrix and performed another nMDS analysis as per above. We
687 also performed a PERMANOVA and visualized the data in the same way as described
688 above, but we did not perform the SIMPER routine due to the lower number of
689 categories. Further, we scaled the size of the symbols to represent the percent of live
690 coral cover. Finally, we statistically compared live coral cover among the two locations
691 using a Bayesian hierarchical model. We logit-transformed proportional *LiveCoralCover*
692 and specified *Location* as a fixed effect, with *Site* specified as a random effect. Model
693 and chain specifications were programmed as described above.

To compare intrinsic temperature tolerances, as derived from CT_{min} and CT_{max} trials, we ran two separate Bayesian linear models. For both models, we specified an effect of *Population* (i.e., separate levels for each species and their respective Arabian Gulf and Gulf of Oman populations) on the critical thermal limit of individuals and examined differences between pairwise levels using post-hoc contrasts (Tables S2 and S3). Models were run with a Gaussian error distribution and the same specifications as the previous models (e.g., burnin, iterations, priors, etc.). We took 1,000 draws from the posterior parameters to fit posterior distributions as well as their mean and confidence bands and plotted them alongside the raw data. Furthermore, to examine location-specific differences in length-weight relationships and species-specific abundances, we isolated individuals from three species (*C. anomolus*, *E. pulcher*, and *E. ventermaculus*) and ran separate models for each species to test the effects of total length (*TL*) and *Location* on *Weight*, with log-transformations of both *Weight* and *TL* and the effect of location (with a random effect of *Site*) on abundance. We used a Gaussian error distribution for the first set of models since the data were continuous and approximately normally distributed. We used a negative binomial error distribution for the second set of models since the data were non-negative integers and over-dispersed when run under a Poisson distribution. To validate the model performance, we used the posterior parameters to predict values across a sequence of 100 evenly spaced values within the sampled size range of the two populations. We performed this 500 times and plotted each predicted model fit alongside the raw data. Models were run with the same prior and chain specifications as detailed above.

We examined prey item ingestion of the examined fishes using a network theory approach for both the COI and 23S markers¹²¹. We first created a presence-absence matrix of OTUs/ESVs across fish individuals in all species and their populations, creating a bipartite dietary network based on prey presence or absence. To examine the community structure within the network, we omitted all prey items with only a single occurrence across the dataset since the full dataset identified the majority of individuals as unique modules. This step reduced the COI dataset from 1,357 to 1,046 unique predator-prey interactions and the 23S dataset from 7,872 to 5,698 predator-prey interactions. We then sought to identify modules within the network using Newman's modularity measure¹²². We used Beckett's community detection algorithm¹²³, which we re-iterated 20 times for each dataset. We then used the convergent output from the 20 iterations to determine the module membership of each individual in our network. We then created a data frame from the original presence-absence matrix that contained each OTU/ESV and its linkage to the fish individual in two columns, which we then summarized by the respective modules. This created a list of symbolic edges in the network across the two columns, linking each prey item to a module, which we plotted as a bipartite dietary network tree using the Fruchterman-Reingold algorithm. We also plotted module membership in a mosaic plot.

Furthermore, for the COI and 23S markers, we investigated prey item diversity ingested by each species' population by producing interpolated and extrapolated rarefaction curves, which showcase sequencing depth by plotting prey item species richness by the total number of sequences detected for each species. We ran rarefaction analyses by rarefying species richness estimates for each species or

population to an endpoint defined by the maximum sequences in any population using 100 bootstraps and 50 knots along the x-axis¹²⁴.

Finally, we modelled growth and mortality dynamics in cryptobenthic fish assemblages from the two locations, ultimately yielding a standing biomass estimate and three rate-based metrics that serve as indicators of energy and nutrient fluxes, thus indicating ecosystem functioning²⁵: produced biomass (in g d⁻¹m⁻²), consumed biomass (in g d⁻¹m⁻²), and total turnover (percent d⁻¹)^{94,125,126}. Produced biomass represents the amount of fish tissue accumulated by an assemblage (in this case, a cryptobenthic fish assemblage collected in a given sample), thus considering only the growth that will occur on any given day (based on yearly averages in this case). Consumed biomass represents the amount of fish tissue that perished based on our estimates of fish mortality. In this pathway, the energy and nutrients produced by fishes are provided to other consumers or decomposers via predation or detritivory. Finally, total turnover expands on the classic estimate of turnover (the production/standing biomass [P/B] ratio¹²⁷) by also including consumed biomass (consumed biomass/standing biomass)¹²⁵. As such, the turnover metric approximates the rate at which particles flow through the system, either via incorporation into fish biomass or release to other consumers through mortality.

For the modeling, we first accrued species-specific information on maximum lengths and a range of coarse ecological traits (pertaining to diet, sociality, habitat association, and prevailing mean sea surface temperatures [SST]) from the literature for each species in our samples. We also extracted length-weight relationships at the family-level, since not all species in our samples were common enough to construct

robust length-weight relationships. We then used these data to calculate species-specific growth coefficients (K_{\max}) to the specified maximum size and modeled individual weight gain based on changes in fish size per day under a Von Bertalanffy Growth Model (VBGM)¹²⁶. By subtracting the observed fish size (as obtained from our samples) from the weight obtained by the same fish after one day (from the model), we calculated the expected biomass production by that individual. We estimated daily mortality rates by calculating species-level mortality risk coefficients via VBGM parameters and SST^{125,128}, and then we adjusted the risk based on relationships between mortality and body size¹²⁹. Using these coefficients, we obtained a daily survival probability for a given individual in the dataset. By combining this probability with biomass production as obtained from the previous step, we were able to generate the expected loss of biomass due to natural mortality at the individual level. Finally, we summed the individual-level estimates of weight, growth, and mortality for each sample to obtain community-level values of standing biomass, produced biomass, and consumed biomass, which we used to calculate total turnover as the combined quotients of produced and consumed biomass and standing biomass.

All data preparation, analyses, and visualizations were performed in *R*¹³⁰ (version 3.6.1) using the *tidyverse*¹³¹, *vegan*¹³², *brms*¹²⁰, *iNEXT*¹²⁴, *igraph*¹³³, *bipartite*¹³⁴, *tidybayes*¹³⁵, *xgboost*¹³⁶, *emmeans*¹³⁷, *oceanmap*¹³⁸, *ncdf4*¹³⁹ and *raster*¹⁴⁰ packages. All graphs were made using the *Trimma lantana* and *Coryphaena hippurus* color palettes in the package *fishualize*¹⁴¹. Growth modeling was performed using a beta version of the package *rfishprod*.

784 References

- 785 1. Dornelas, M. *et al.* Assemblage time series reveal biodiversity change but not systematic loss.
786 *Science* **344**, 296–299 (2014).
- 787 2. Blowes, S. A. *et al.* The geography of biodiversity change in marine and terrestrial assemblages.
788 *Science* **366**, 339–345 (2019).
- 789 3. Johnson, C. N. *et al.* Biodiversity losses and conservation responses in the Anthropocene. *Science*
790 **356**, 270–275 (2017).
- 791 4. Mace, G. M., Norris, K. & Fitter, A. H. Biodiversity and ecosystem services: a multilayered
792 relationship. *Trends in ecology & evolution* **27**, 19–26 (2012).
- 793 5. Vellend, M. *The theory of ecological communities (MPB-57)*. vol. 75 (Princeton University Press,
794 2016).
- 795 6. Kraft, N. J. *et al.* Community assembly, coexistence and the environmental filtering metaphor.
796 *Functional Ecology* **29**, 592–599 (2015).
- 797 7. Kraft, N. J., Valencia, R. & Ackerly, D. D. Functional traits and niche-based tree community assembly
798 in an Amazonian forest. *Science* **322**, 580–582 (2008).
- 799 8. Leibold, M. A. *et al.* The metacommunity concept: a framework for multi-scale community ecology.
800 *Ecology letters* **7**, 601–613 (2004).
- 801 9. Cardinale, B. J. *et al.* Biodiversity loss and its impact on humanity. *Nature* **486**, 59–67 (2012).
- 802 10. Duffy, J. E., Godwin, C. M. & Cardinale, B. J. Biodiversity effects in the wild are common and as
803 strong as key drivers of productivity. *Nature* **549**, 261 (2017).
- 804 11. Schweiger, A. K. *et al.* Plant spectral diversity integrates functional and phylogenetic components of
805 biodiversity and predicts ecosystem function. *Nature ecology & evolution* **2**, 976 (2018).
- 806 12. Pecl, G. T. *et al.* Biodiversity redistribution under climate change: Impacts on ecosystems and human
807 well-being. *Science* **355**, eaai9214 (2017).
- 808 13. Scheffers, B. R. *et al.* The broad footprint of climate change from genes to biomes to people. *Science*
809 **354**, aaf7671 (2016).
- 810 14. García, F. C., Bestion, E., Warfield, R. & Yvon-Durocher, G. Changes in temperature alter the
811 relationship between biodiversity and ecosystem functioning. *Proceedings of the National Academy*
812 *of Sciences* **115**, 10989–10994 (2018).
- 813 15. Pörtner, H. O. & Farrell, A. P. Physiology and climate change. *Science* **322**, 690–692 (2008).
- 814 16. Deutsch, C., Ferrel, A., Seibel, B., Pörtner, H.-O. & Huey, R. B. Climate change tightens a metabolic
815 constraint on marine habitats. *Science* **348**, 1132–1135 (2015).
- 816 17. Bozinovic, F. & Pörtner, H. Physiological ecology meets climate change. *Ecology and evolution* **5**,
817 1025–1030 (2015).
- 818 18. Barneche, D. R., Jahn, M. & Seebacher, F. Warming increases the cost of growth in a model
819 vertebrate. *Functional Ecology*.
- 820 19. Brown, J. H., Hall, C. A. & Sibly, R. M. Equal fitness paradigm explained by a trade-off between
821 generation time and energy production rate. *Nature ecology & evolution* **2**, 262 (2018).
- 822 20. Toseland, A. *et al.* The impact of temperature on marine phytoplankton resource allocation and
823 metabolism. *Nature Climate Change* **3**, 979 (2013).
- 824 21. Barneche, D. R. & Allen, A. P. The energetics of fish growth and how it constrains food-web trophic
825 structure. *Ecology letters* **21**, 836–844 (2018).
- 826 22. Gardner, J. L., Peters, A., Kearney, M. R., Joseph, L. & Heinsohn, R. Declining body size: a third
827 universal response to warming? *Trends in ecology & evolution* **26**, 285–291 (2011).
- 828 23. Chesson, P. Mechanisms of maintenance of species diversity. *Annual review of Ecology and*
829 *Systematics* **31**, 343–366 (2000).
- 830 24. Barnes, A. D. *et al.* Energy flux: the link between multitrophic biodiversity and ecosystem functioning.
831 *Trends in ecology & evolution* **33**, 186–197 (2018).

25. Brandl, S. J. *et al.* Coral reef ecosystem functioning: eight core processes and the role of biodiversity. *Frontiers in Ecology and the Environment* (2019).
26. Spalding, M. *et al.* Mapping the global value and distribution of coral reef tourism. *Marine Policy* **82**, 104–113 (2017).
27. Hughes, T. P. *et al.* Spatial and temporal patterns of mass bleaching of corals in the Anthropocene. *Science* **359**, 80–83 (2018).
28. Pratchett, M. S., Hoey, A. S., Wilson, S. K., Messmer, V. & Graham, N. A. Changes in biodiversity and functioning of reef fish assemblages following coral bleaching and coral loss. *Diversity* **3**, 424–452 (2011).
29. Brandl, S. J., Emslie, M. J. & Ceccarelli, D. M. Habitat degradation increases functional originality in highly diverse coral reef fish assemblages. *Ecosphere* **7**, (2016).
30. Fontoura, L. *et al.* Climate-driven shift in coral morphological structure predicts decline of juvenile reef fishes. *Global change biology* (2019).
31. Bellwood, D. R., Hoey, A. S., Ackerman, J. L. & Depczynski, M. Coral bleaching, reef fish community phase shifts and the resilience of coral reefs. *Global Change Biology* **12**, 1587–1594 (2006).
32. Robinson, J. P. *et al.* Productive instability of coral reef fisheries after climate-driven regime shifts. *Nature ecology & evolution* **3**, 183 (2019).
33. Wismer, S., Tebbett, S. B., Streit, R. P. & Bellwood, D. R. Young fishes persist despite coral loss on the Great Barrier Reef. *Communications Biology* **2**, 456 (2019).
34. Taylor, B. M. *et al.* Synchronous biological feedbacks in parrotfishes associated with pantropical coral bleaching. *Global Change Biology* (2019).
35. Pörtner, H. O. & Knust, R. Climate change affects marine fishes through the oxygen limitation of thermal tolerance. *science* **315**, 95–97 (2007).
36. Comte, L. & Olden, J. D. Climatic vulnerability of the world's freshwater and marine fishes. *Nature Climate Change* **7**, 718 (2017).
37. Munday, P. L., McCormick, M. I. & Nilsson, G. E. Impact of global warming and rising CO₂ levels on coral reef fishes: what hope for the future? *Journal of Experimental Biology* **215**, 3865–3873 (2012).
38. Munday, P. L., Jones, G. P., Pratchett, M. S. & Williams, A. J. Climate change and the future for coral reef fishes. *Fish and Fisheries* **9**, 261–285 (2008).
39. Donelson, J., Munday, P., McCormick, M. & Pitcher, C. Rapid transgenerational acclimation of a tropical reef fish to climate change. *Nature Climate Change* **2**, 30 (2012).
40. Johansen, J. & Jones, G. Increasing ocean temperature reduces the metabolic performance and swimming ability of coral reef damselfishes. *Global Change Biology* **17**, 2971–2979 (2011).
41. Rummer, J. L. *et al.* Life on the edge: thermal optima for aerobic scope of equatorial reef fishes are close to current day temperatures. *Global change biology* **20**, 1055–1066 (2014).
42. Nilsson, G. E., Crawley, N., Lunde, I. G. & Munday, P. L. Elevated temperature reduces the respiratory scope of coral reef fishes. *Global Change Biology* **15**, 1405–1412 (2009).
43. Eme, J. & Bennett, W. A. Critical thermal tolerance polygons of tropical marine fishes from Sulawesi, Indonesia. *Journal of Thermal Biology* **34**, 220–225 (2009).
44. Gardiner, N. M., Munday, P. L. & Nilsson, G. E. Counter-gradient variation in respiratory performance of coral reef fishes at elevated temperatures. *PLoS One* **5**, e13299 (2010).
45. Mora, C. & Ospina, A. Tolerance to high temperatures and potential impact of sea warming on reef fishes of Gorgona Island (tropical eastern Pacific). *Marine Biology* **139**, 765–769 (2001).
46. Feary, D. A. *et al.* Latitudinal shifts in coral reef fishes: why some species do and others do not shift. *Fish and Fisheries* **15**, 593–615 (2014).
47. Bernal, M. A. *et al.* Phenotypic and molecular consequences of stepwise temperature increase across generations in a coral reef fish. *Molecular Ecology* **27**, 4516–4528 (2018).
48. Grenchik, M., Donelson, J. & Munday, P. Evidence for developmental thermal acclimation in the damselfish, *Pomacentrus moluccensis*. *Coral Reefs* **32**, 85–90 (2013).

49. Miller, D. D., Ota, Y., Sumaila, U. R., Cisneros-Montemayor, A. M. & Cheung, W. W. Adaptation strategies to climate change in marine systems. *Global change biology* **24**, e1–e14 (2018).
50. Brandl, S. J., Goatley, C. H., Bellwood, D. R. & Tornabene, L. The hidden half: ecology and evolution of cryptobenthic fishes on coral reefs. *Biological Reviews* **93**, 1846–1873 (2018).
51. Brandl, S. J., Casey, J. M., Knowlton, N. & Duffy, J. E. Marine dock pilings foster diverse, native cryptobenthic fish assemblages across bioregions. *Ecology and evolution* **7**, 7069–7079 (2017).
52. Ahmadi, G. N., Tornabene, L., Smith, D. J. & Pezold, F. L. The relative importance of regional, local, and evolutionary factors structuring cryptobenthic coral-reef assemblages. *Coral Reefs* **37**, 279–293 (2018).
53. Coker, D. J., DiBattista, J. D., Sinclair-Taylor, T. H. & Berumen, M. L. Spatial patterns of cryptobenthic coral-reef fishes in the Red Sea. *Coral Reefs* 1–7 (2017).
54. Brandl, S. J. *et al.* Demographic dynamics of the smallest marine vertebrates fuel coral reef ecosystem functioning. *Science* **364**, 1189–1192 (2019).
55. Miller, P. J. Miniature vertebrates. The implications of small body size. in vol. 69 (Oxford University Press, 1996).
56. Depczynski, M. & Bellwood, D. Microhabitat utilisation patterns in cryptobenthic coral reef fish communities. *Marine Biology* **145**, 455–463 (2004).
57. Bellwood, D. R. *et al.* Coral recovery may not herald the return of fishes on damaged coral reefs. *Oecologia* **170**, 567–573 (2012).
58. Depczynski, M. & Bellwood, D. R. Shortest recorded vertebrate lifespan found in a coral reef fish. *Current Biology* **15**, R288–R289.
59. Tornabene, L., Valdez, S., Erdmann, M. & Pezold, F. Support for a ‘Center of Origin’ in the Coral Triangle: Cryptic diversity, recent speciation, and local endemism in a diverse lineage of reef fishes (Gobiidae: Eviota). *Molecular phylogenetics and evolution* **82**, 200–210 (2015).
60. Price, A., Sheppard, C. & Roberts, C. The Gulf: its biological setting. *Marine Pollution Bulletin* **27**, 9–15 (1993).
61. Riegl, B. M. & Purkis, S. J. Coral reefs of the Gulf: adaptation to climatic extremes in the world’s hottest sea. in *Coral reefs of the Gulf* 1–4 (Springer, 2012).
62. Eagderi, S., Fricke, R., Esmaeili, H. & Jalili, P. Annotated checklist of the fishes of the Persian Gulf: Diversity and conservation status. *Iranian Journal of Ichthyology* **6**, 1–171 (2019).
63. Casey, J. M. *et al.* Reconstructing hyperdiverse food webs: Gut content metabarcoding as a tool to disentangle trophic interactions on coral reefs. *Methods in Ecology and Evolution* **10**, 1157–1170 (2019).
64. Depczynski, M. & Bellwood, D. R. The role of cryptobenthic reef fishes in coral reef trophodynamics. *Marine Ecology Progress Series* **256**, 183–191 (2003).
65. Pratchett, M. S., Wilson, S. K. & Munday, P. L. 13 Effects of climate change on coral reef fishes. *Ecology of fishes on coral reefs* 127 (2015).
66. Purkis, S. J. & Riegl, B. M. Geomorphology and Reef Building in the SE Gulf. in *Coral Reefs of the Gulf: Adaptation to Climatic Extremes* (eds. Riegl, B. M. & Purkis, S. J.) 33–50 (Springer Netherlands, 2012). doi:10.1007/978-94-007-3008-3_3.
67. Krupp, F. & Müller, T. The status of fish populations in the northern Arabian Gulf two years after the 1991 Gulf War oil spill. *Courier Forschungsinst Senckenb* **166**, 67–75 (1994).
68. Bishop, J. History and current checklist of Kuwait’s ichthyofauna. *Journal of Arid Environments* **54**, 237–256 (2003).
69. Donelson, J. M., Munday, P. L., McCORMICK, M. I. & Nilsson, G. E. Acclimation to predicted ocean warming through developmental plasticity in a tropical reef fish. *Global Change Biology* **17**, 1712–1719 (2011).
70. Ohlberger, J. Climate warming and ectotherm body size—from individual physiology to community ecology. *Functional Ecology* **27**, 991–1001 (2013).

71. Peig, J. & Green, A. J. The paradigm of body condition: a critical reappraisal of current methods based on mass and length. *Functional Ecology* **24**, 1323–1332 (2010).
72. Sullam, K. E. *et al.* Changes in digestive traits and body nutritional composition accommodate a trophic niche shift in Trinidadian guppies. *Oecologia* **177**, 245–257 (2015).
73. Whelan, C. J., Brown, J. S., Schmidt, K. A., Steele, B. B. & Willson, M. F. Linking consumer–resource theory and digestive physiology: application to diet shifts. *Evolutionary Ecology Research* **2**, 911–934 (2000).
74. Petchey, O. L. Prey diversity, prey composition, and predator population dynamics in experimental microcosms. *Journal of Animal Ecology* **69**, 874–882 (2000).
75. Merrick, R. L., Chumbley, M. K. & Byrd, G. V. Diet diversity of Steller sea lions (*Eumetopias jubatus*) and their population decline in Alaska: a potential relationship. *Can. J. Fish. Aquat. Sci.* **54**, 1342–1348 (1997).
76. Hondorp, D. W., Pothoven, S. A. & Brandt, S. B. Influence of *Diporeia* density on diet composition, relative abundance, and energy density of planktivorous fishes in southeast Lake Michigan. *Transactions of the American fisheries Society* **134**, 588–601 (2005).
77. Shraim, R. *et al.* Environmental Extremes Are Associated with Dietary Patterns in Arabian Gulf Reef Fishes. *Frontiers in Marine Science* **4**, 285 (2017).
78. Agorreta, A. *et al.* Molecular phylogenetics of Gobioidae and phylogenetic placement of European gobies. *Molecular Phylogenetics and Evolution* **69**, 619–633 (2013).
79. Thacker, C. E. & Roje, D. M. Phylogeny of Gobiidae and identification of gobiid lineages. *Systematics and Biodiversity* **9**, 329–347 (2011).
80. Kovačić, M., Bogorodsky, S. V. & Mal, A. O. Two new species of *Coryogalops* (Perciformes: Gobiidae) from the Red Sea. *Zootaxa* **3881**, 513–531 (2014).
81. Rishworth GM, Strydom NA & Perissinotto R. Fishes associated with living stromatolite communities in peritidal pools: predators, recruits and ecological traps. *Mar Ecol Prog Ser* **580**, 153–167 (2017).
82. Munday, P. L. & Jones, G. P. The ecological implications of small body size among coral-reef fishes. *Oceanogr Mar Biol Annu Rev* **36**, 373–411 (1998).
83. Sandblom, E. *et al.* Physiological constraints to climate warming in fish follow principles of plastic floors and concrete ceilings. *Nature communications* **7**, 11447 (2016).
84. Norin, T. & Metcalfe, N. B. Ecological and evolutionary consequences of metabolic rate plasticity in response to environmental change. *Philosophical Transactions of the Royal Society B* **374**, 20180180 (2019).
85. Sheldon, K. S., Yang, S. & Tewksbury, J. J. Climate change and community disassembly: impacts of warming on tropical and temperate montane community structure. *Ecology Letters* **14**, 1191–1200 (2011).
86. Crossland, C., Hatcher, B. & Smith, S. Role of coral reefs in global ocean production. *Coral reefs* **10**, 55–64 (1991).
87. Gove, J. M. *et al.* Near-island biological hotspots in barren ocean basins. *Nature communications* **7**, 10581 (2016).
88. De Goeij, J. M. *et al.* Surviving in a marine desert: the sponge loop retains resources within coral reefs. *Science* **342**, 108–110 (2013).
89. Wild, C. *et al.* Coral mucus functions as an energy carrier and particle trap in the reef ecosystem. *Nature* **428**, 66–70 (2004).
90. Hamner, W., Jones, M., Carleton, J., Hauri, I. & Williams, D. M. Zooplankton, planktivorous fish, and water currents on a windward reef face: Great Barrier Reef, Australia. *Bulletin of Marine Science* **42**, 459–479 (1988).
91. Hatcher, B. G. Coral reef primary productivity: a beggar's banquet. *Trends in Ecology & Evolution* **3**, 106–111 (1988).

92. Bacon, P., Gurney, W., Jones, W., McLaren, I. & Youngson, A. Seasonal growth patterns of wild juvenile fish: partitioning variation among explanatory variables, based on individual growth trajectories of Atlantic salmon (*Salmo salar*) parr. *Journal of Animal Ecology* **74**, 1–11 (2005).
93. Coles, S. L. Coral species diversity and environmental factors in the Arabian Gulf and the Gulf of Oman: a comparison to the Indo-Pacific region. *Atoll Research Bulletin* (2003).
94. Morais, R. A. & Bellwood, D. R. Pelagic Subsidies Underpin Fish Productivity on a Degraded Coral Reef. *Current Biology* **29**, 1521–1527 (2019).
95. Riegl, B. Effects of the 1996 and 1998 positive sea-surface temperature anomalies on corals, coral diseases and fish in the Arabian Gulf (Dubai, UAE). *Marine biology* **140**, 29–40 (2002).
96. Riegl, B. & Purkis, S. Coral population dynamics across consecutive mass mortality events. *Global change biology* **21**, 3995–4005 (2015).
97. Burt, J., Al-Harhi, S. & Al-Cibahy, A. Long-term impacts of coral bleaching events on the world's warmest reefs. *Marine environmental research* **72**, 225–229 (2011).
98. Burt, J. A., Paparella, F., Al-Mansoori, N., Al-Mansoori, A. & Al-Jailani, H. Causes and consequences of the 2017 coral bleaching event in the southern Persian/Arabian Gulf. *Coral Reefs* **38**, 567–589 (2019).
99. Coker, D. J., Wilson, S. K. & Pratchett, M. S. Importance of live coral habitat for reef fishes. *Reviews in Fish Biology and Fisheries* **24**, 89–126 (2014).
100. Pratchett, M. S., Baird, A. H., Bauman, A. G. & Burt, J. A. Abundance and composition of juvenile corals reveals divergent trajectories for coral assemblages across the United Arab Emirates. *Marine Pollution Bulletin* **114**, 1031–1035 (2017).
101. Munday, P. L. Habitat loss, resource specialization, and extinction on coral reefs. *Global Change Biology* **10**, 1642–1647 (2004).
102. Burt, J. A. *et al.* Biogeographic patterns of reef fish community structure in the northeastern Arabian Peninsula. *ICES Journal of Marine Science* **68**, 1875–1883 (2011).
103. Feary, D. A., Burt, J. A., Cavalcante, G. H. & Bauman, A. G. Extreme Physical Factors and the Structure of Gulf Fish and Reef Communities. in *Coral Reefs of the Gulf: Adaptation to Climatic Extremes* (eds. Riegl, B. M. & Purkis, S. J.) 163–170 (Springer Netherlands, 2012). doi:10.1007/978-94-007-3008-3_9.
104. Brose, U. *et al.* Predator traits determine food-web architecture across ecosystems. *Nature ecology & evolution* **3**, 919 (2019).
105. Ackerman, J. L. & Bellwood, D. R. Reef fish assemblages: a re-evaluation using enclosed rotenone stations. *Marine Ecology-Progress Series* **206**, 227–237 (2000).
106. Beitinger, T. L., Bennett, W. A. & McCauley, R. W. Temperature tolerances of North American freshwater fishes exposed to dynamic changes in temperature. *Environmental biology of fishes* **58**, 237–275 (2000).
107. Leray, M. *et al.* A new versatile primer set targeting a short fragment of the mitochondrial COI region for metabarcoding metazoan diversity: application for characterizing coral reef fish gut contents. *Frontiers in zoology* **10**, 34 (2013).
108. Geller, J., Meyer, C., Parker, M. & Hawk, H. Redesign of PCR primers for mitochondrial cytochrome c oxidase subunit I for marine invertebrates and application in all-taxa biotic surveys. *Molecular ecology resources* **13**, 851–861 (2013).
109. Sherwood, A. R. & Presting, G. G. Universal primers amplify a 23S rDNA plastid marker in eukaryotic algae and cyanobacteria. *Journal of phycology* **43**, 605–608 (2007).
110. Hamsher, S. E., Evans, K. M., Mann, D. G., Poulíčková, A. & Saunders, G. W. Barcoding diatoms: exploring alternatives to COI-5P. *Protist* **162**, 405–422 (2011).
111. Cannon, M. *et al.* In silico assessment of primers for eDNA studies using PrimerTree and application to characterize the biodiversity surrounding the Cuyahoga River. *Scientific reports* **6**, 22908 (2016).

112. Caporaso, J. G. *et al.* QIIME allows analysis of high-throughput community sequencing data. *Nature methods* **7**, 335 (2010).
113. Edgar, R. C. UPARSE: highly accurate OTU sequences from microbial amplicon reads. *Nature methods* **10**, 996 (2013).
114. Martin, M. Cutadapt removes adapter sequences from high-throughput sequencing reads. *EMBnet. journal* **17**, 10–12 (2011).
115. Edgar, R. C. Search and clustering orders of magnitude faster than BLAST. *Bioinformatics* **26**, 2460–2461 (2010).
116. Camacho, C. *et al.* BLAST+: architecture and applications. *BMC bioinformatics* **10**, 421 (2009).
117. Edgar, R. C. & Flyvbjerg, H. Error filtering, pair assembly and error correction for next-generation sequencing reads. *Bioinformatics* **31**, 3476–3482 (2015).
118. Edgar, R. C. UNOISE2: improved error-correction for Illumina 16S and ITS amplicon sequencing. *BioRxiv* 081257 (2016).
119. Yilmaz, P. *et al.* The SILVA and “all-species living tree project (LTP)” taxonomic frameworks. *Nucleic acids research* **42**, D643–D648 (2013).
120. Bürkner, P.-C. Advanced Bayesian Multilevel Modeling with the R Package brms. *arXiv preprint arXiv:1705.11123* (2017).
121. Wasserman, S. & Faust, K. *Social network analysis: Methods and applications*. vol. 8 (Cambridge university press, 1994).
122. Newman, M. E. Modularity and community structure in networks. *Proceedings of the national academy of sciences* **103**, 8577–8582 (2006).
123. Beckett, S. J. Improved community detection in weighted bipartite networks. *Royal Society open science* **3**, 140536 (2016).
124. Hsieh, T., Ma, K. & Chao, A. iNEXT: an R package for rarefaction and extrapolation of species diversity (Hill numbers). *Methods in Ecology and Evolution* (2016).
125. Brandl, S. J. *et al.* Supplemental Materials for Demographic dynamics of the smallest marine vertebrates fuel coral reef ecosystem functioning. *Science* **364**, 1189–1192 (2019).
126. Morais, R. A. & Bellwood, D. R. Global drivers of reef fish growth. *Fish and Fisheries*.
127. Allen, K. R. Relation between production and biomass. *Journal of the Fisheries Board of Canada* **28**, 1573–1581 (1971).
128. Pauly, D. On the interrelationships between natural mortality, growth parameters, and mean environmental temperature in 175 fish stocks. *ICES Journal of Marine Science* **39**, 175–192 (1980).
129. Gislason, H., Daan, N., Rice, J. C. & Pope, J. G. Size, growth, temperature and the natural mortality of marine fish. *Fish and Fisheries* **11**, 149–158 (2010).
130. R Core Team. *R: A language and environment for statistical computing*. (2019).
131. Wickham, H. Tidyverse: Easily install and load ‘tidyverse’ packages. *R package version 1*, (2017).
132. Oksanen, J. *et al.* The vegan package. *Community ecology package* **10**, (2007).
133. Csardi, G. & Nepusz, T. The igraph software package for complex network research. *InterJournal, Complex Systems* **1695**, 1–9 (2006).
134. Dormann, C. F., Gruber, B. & Fründ, J. Introducing the bipartite package: analysing ecological networks. *interaction* **1**, (2008).
135. Kay, M. tidybayes: Tidy data and geoms for Bayesian models. *R package version 1*, (2018).
136. Chen, T., He, T., Benesty, M., Khotilovich, V. & Tang, Y. Xgboost: extreme gradient boosting. *R package version 0.4-2* 1–4 (2015).
137. Lenth, R., Singmann, H., Love, J., Buerkner, P. & Herve, M. Package “emmeans”: Estimated marginal means, aka least-squares means. *Compr. R Arch. Netw* 1–67 (2019).
138. Bauer, R. Oceanmap: a plotting toolbox for 2D oceanographic data. *R package, version 0.0.9*, (2017).
139. Pierce, D. & Pierce, M. D. Package ‘ncdf4’. (2019).

1076 140. Hijmans, R. J. *et al.* Raster package in R. (2013).
1077 141. Schiettekatte, N. M., Brandl, S. J. & Casey, J. M. *fishualize: Color palettes based on fish species*.
1078 (2019).
1079
1080
1081

Acknowledgments

We thank the Environment Agency Abu Dhabi (TMBS/18/L/179) and Dibba Municipality (unnumbered) for collection permits and the UAE Ministry of Environment and Climate Change for the tissue export permit (AUD-Q-22-1110520). All work was performed under NYUAD IACUC approval 18-0003. We further thank the NYU Abu Dhabi Center for Genomics and Systems Biology for sequencing funding and the NYU Abu Dhabi Core Facilities group for support of field collections and thermal experiments. We thank Dain McParland and Grace Vaughan for field support, Noura Al-Mansoori for assistance with processing specimens in the laboratory, and Katherine Maslenikov and Jonathon Huie for assistance in cataloging specimens at the University of Washington. Partial fieldwork funding was provided to L Tornabene by the University of Washington.

Author contributions

SJB and JLJ designed the study; SJB, JLJ, JMC, and LT performed field collections; JLJ ran physiological trials; SJB, JMC, and LT performed laboratory work; JAB and LT provided funding and resources; SJB performed data analysis and visualization; SJB and RAM performed population modeling; SJB wrote the first draft of the manuscript, and all authors contributed to writing thereafter.

Data accessibility and conflicts of interest

All data and code necessary to produce the results are included in this submission and will be made public upon publication of the paper. We declare no conflict of interest.

1105 **Supplemental Material**

1106 **Table S1| Presence, abundance, and previous records of species sampled in the**
 1107 **present study.** Each row represents a species, with columns AG (Arabian Gulf) and
 1108 GO (Gulf of Oman) indicating the abundance of the species in our samples. Column *R*
 1109 indicates whether the species has been previously recorded in other parts of the
 1110 Arabian Gulf (* = yes, – = no). References for previous records are provided.
 1111

<i>Family</i>	<i>Species</i>	<i>AG</i>	<i>GO</i>	<i>R</i>	<i>Reference</i>
Apogonidae	<i>Apogon coccineus</i>	6	10	*	present
Apogonidae	<i>Apogonichthyoides taeniatus</i>	2	0	*	present
Apogonidae	<i>Cheilodipterus novemstriatus</i>	2	9	*	present
Apogonidae	<i>Cheilodipterus persicus</i>	0	1	*	Krupp & Müller 1994
Apogonidae	<i>Fowleria variegata</i>	5	1	*	present
Apogonidae	<i>Ostorhinchus cyanosoma</i>	0	15	*	Krupp & Müller 1994
Apogonidae	<i>Ostorhinchus fleurieu</i>	0	30	*	Eagderi et al. 2019
Batrachoididae	<i>Colletteichthys occidentalis</i>	6	0	*	present
Blenniidae	<i>Antennablennius adenensis</i>	0	54	*	Bishop 2003
Blenniidae	<i>Ecsenius pulcher</i>	8	97	*	present
Blenniidae	<i>Laiphognathus multimaculatus</i>	1	0	*	present
Bythitidae	<i>Dinematichthys iluocoeteoides</i>	5	0	*	present
Gobiidae	<i>Asterropteryx semipunctata</i>	0	2	*	Krupp & Müller 1994
Gobiidae	<i>Callogobius bifasciatus</i>	2	0	*	present
Gobiidae	<i>Callogobius speA</i>	0	3	*	Eagderi et al. 2019
Gobiidae	<i>Coryogalops anomalus</i>	65	33	*	present
Gobiidae	<i>Eviota guttata</i>	0	69	*	Krupp & Müller 1994
Gobiidae	<i>Eviota punyit</i>	0	12	*	Krupp & Müller 1994 ₁
Gobiidae	<i>Favonigobius melanobranchus</i>	1	0	*	present
Gobiidae	<i>Fusigobius inframaculatus</i>	0	3	*	Eagderi et al. 2019
Gobiidae	<i>Gnatholepis caudimaculata</i>	0	14	*	Eagderi et al. 2019
Gobiidae	<i>Gobiodon reticulatus</i>	0	2	*	Bishop 2003
Gobiidae	<i>Heteroleotris vulgaris</i>	0	405	*	Eagderi et al. 2019
Gobiidae	<i>Istigobius decoratus</i>	0	15	*	Eagderi et al. 2019
Gobiidae	<i>Priolepis cincta</i>	0	4	*	Winterbottom & Burridge 1992
Gobiidae	<i>Priolepis randalli</i>	0	2	*	Winterbottom & Burridge 1993
Gobiidae	<i>Priolepis semidoliata</i>	0	10	–	NA
Gobiidae	<i>Trimma corallinum</i>	0	11	*	Eagderi et al. 2019 ₂
Muraenidae	<i>Gymnothorax speA</i>	0	12	*	Eagderi et al. 2019 ₃
Ostraciidae	<i>Ostracion cubicus</i>	0	3	*	Eagderi et al. 2019
Pomacanthidae	<i>Pomacanthus maculosus</i>	7	0	*	present
Pomacentridae	<i>Chromis flavaxilla</i>	0	19	*	Bishop 2003
Pomacentridae	<i>Chromis xanthopterygius</i>	0	3	*	Bishop 2003
Pomacentridae	<i>Neopomacentrus cyanomos</i>	0	38	*	Bishop 2003
Pomacentridae	<i>Neopomacentrus miryae</i>	0	38	–	NA
Pomacentridae	<i>Neopomacentrus sindensis</i>	0	6	*	Bishop 2003
Pomacentridae	<i>Pomacentrus aquilus</i>	3	0	*	present
Pomacentridae	<i>Pomacentrus leptus</i>	0	5	*	Bishop 2003
Pomacentridae	<i>Pomacentrus trichourus</i>	5	0	*	present
Pseudochromidae	<i>Pseudochromis aldabraensis</i>	0	4	*	Bishop 2003

Pseudochromidae	<i>Pseudochromis linda</i>	1	0	*	present
Pseudochromidae	<i>Pseudochromis nigrovittatus</i>	2	1	*	present
Pseudochromidae	<i>Pseudochromis persicus</i>	1	0	*	present
Serranidae	<i>Cephalopholis hemistiktos</i>	2	2	*	present
Syngnathidae	<i>Corythoichthys flavofasciata</i>	0	5	*	Froese & Pauly 2019
Syngnathidae	<i>Doryrhamphus excisus</i>	0	3	*	Bishop 2003
Tripterygiidae	<i>Enneapterygius ventermaculus</i>	131	262	*	present
Tripterygiidae	<i>Helcogramma fuscopinna</i>	0	134	—	NA

¹identified as *E. sebreei*

²synonymous with *T. winterbottomi*

³genus level

Table S2 | Contrasts between levels of the explanatory variable for the model testing CT_{max} differences in cryptobenthic reef fishes. Population columns highlight the contrast estimated in the model, whereas the estimate and its confidence intervals indicate estimated differences.

Population I	Population II	Estimate	LCI	UCI
<i>C. anomolus</i> .AG	<i>E. pulcher</i> .AG	0.486	-0.079	1.054
<i>C. anomolus</i> .AG	<i>E. ventermaculus</i> .AG	1.360	0.808	1.949
<i>C. anomolus</i> .AG	<i>E. pulcher</i> .GoO	1.114	0.581	1.726
<i>C. anomolus</i> .AG	<i>E. ventermaculus</i> .GoO	1.633	0.939	2.342
<i>C. anomolus</i> .AG	<i>E. guttata</i> .GoO	1.143	0.534	1.759
<i>C. anomolus</i> .AG	<i>H. fuscopinna</i> .GoO	2.392	1.758	2.992
<i>C. anomolus</i> .AG	<i>H. vulgaris</i> .GoO	0.492	-0.061	1.078
<i>E. pulcher</i> .AG	<i>E. ventermaculus</i> .AG	0.879	0.509	1.252
<i>E. pulcher</i> .AG	<i>E. pulcher</i> .GoO	0.636	0.244	1.016
<i>E. pulcher</i> .AG	<i>E. ventermaculus</i> .GoO	1.159	0.624	1.737
<i>E. pulcher</i> .AG	<i>E. guttata</i> .GoO	0.656	0.227	1.134
<i>E. pulcher</i> .AG	<i>H. fuscoguttata</i> .GoO	1.905	1.463	2.341
<i>E. pulcher</i> .AG	<i>H. vulgaris</i> .GoO	0.011	-0.368	0.417
<i>E. ventermaculus</i> .AG	<i>E. pulcher</i> .GoO	-0.245	-0.640	0.118
<i>E. ventermaculus</i> .AG	<i>E. ventermaculus</i> .GoO	0.277	-0.260	0.815
<i>E. ventermaculus</i> .AG	<i>E. guttata</i> .GoO	-0.225	-0.680	0.212
<i>E. ventermaculus</i> .AG	<i>H. fuscopinna</i> .GoO	1.024	0.578	1.449
<i>E. ventermaculus</i> .AG	<i>H. vulgaris</i> .GoO	-0.878	-1.265	-0.508
<i>E. pulcher</i> .GoO	<i>E. ventermaculus</i> .GoO	0.519	-0.0290	1.073
<i>E. pulcher</i> .GoO	<i>E. guttata</i> .GoO	0.020	-0.426	0.494
<i>E. pulcher</i> .GoO	<i>H. fuscopinna</i> .GoO	1.274	0.839	1.726
<i>E. pulcher</i> .GoO	<i>H. vulgaris</i> .GoO	-0.628	-1.037	-0.253
<i>E. ventermaculus</i> .GoO	<i>E. guttata</i> .GoO	-0.502	-1.125	0.106
<i>E. ventermaculus</i> .GoO	<i>H. fuscopinna</i> .GoO	0.750	0.130	1.344
<i>E. ventermaculus</i> .GoO	<i>H. vulgaris</i> .GoO	-1.148	-1.710	-0.584
<i>E. guttata</i> .GoO	<i>H. fuscopinna</i> .GoO	1.252	0.735	1.778
<i>E. guttata</i> .GoO	<i>H. vulgaris</i> .GoO	-0.647	-1.094	-0.148
<i>H. fuscopinna</i> .GoO	<i>H. vulgaris</i> .GoO	-1.906	-2.363	-1.449

Table S3 | Contrasts between levels of the explanatory variable for the model testing CT_{min} differences in cryptobenthic reef fishes. Population columns highlight the contrast estimated in the model, whereas the estimate and its confidence intervals indicate estimated differences.

Population I	Population II	Estimate	LCI	UCI
<i>C. anomolus</i> .AG	<i>E. pulcher</i> .AG	0.613	0.173	1.069
<i>C. anomolus</i> .AG	<i>E. ventermaculus</i> .AG	-0.400	-0.851	0.054
<i>C. anomolus</i> .AG	<i>E. pulcher</i> .GoO	0.747	0.316	1.211
<i>C. anomolus</i> .AG	<i>E. ventermaculus</i> .GoO	-1.391	-1.887	-0.888
<i>C. anomolus</i> .AG	<i>E. guttata</i> .GoO	-0.784	-1.241	-0.317
<i>C. anomolus</i> .AG	<i>H. fuscopinna</i> .GoO	-1.235	-1.736	-0.754
<i>C. anomolus</i> .AG	<i>H. vulgaris</i> .GoO	-0.080	-0.549	0.384
<i>E. pulcher</i> .AG	<i>E. ventermaculus</i> .AG	-1.011	-1.313	-0.709
<i>E. pulcher</i> .AG	<i>E. pulcher</i> .GoO	0.137	-0.165	0.446
<i>E. pulcher</i> .AG	<i>E. ventermaculus</i> .GoO	-2.003	-2.402	-1.641
<i>E. pulcher</i> .AG	<i>E. guttata</i> .GoO	-1.394	-1.704	-1.076
<i>E. pulcher</i> .AG	<i>H. fuscopinna</i> .GoO	-1.847	-2.206	-1.489
<i>E. pulcher</i> .AG	<i>H. vulgaris</i> .GoO	-0.694	-1.010	-0.358
<i>E. ventermaculus</i> .AG	<i>E. pulcher</i> .GoO	1.149	0.847	1.459
<i>E. ventermaculus</i> .AG	<i>E. ventermaculus</i> .GoO	-0.990	-1.382	-0.610
<i>E. ventermaculus</i> .AG	<i>E. guttata</i> .GoO	-0.381	-0.706	-0.065
<i>E. ventermaculus</i> .AG	<i>H. fuscopinna</i> .GoO	-0.836	-1.201	-0.475
<i>E. ventermaculus</i> .AG	<i>H. vulgaris</i> .GoO	0.318	-0.016	0.648
<i>E. pulcher</i> .GoO	<i>E. ventermaculus</i> .GoO	-2.138	-2.526	-1.766
<i>E. pulcher</i> .GoO	<i>E. guttata</i> .GoO	-1.530	-1.843	-1.213
<i>E. pulcher</i> .GoO	<i>H. fuscopinna</i> .GoO	-1.985	-2.341	-1.615
<i>E. pulcher</i> .GoO	<i>H. vulgaris</i> .GoO	-0.832	-1.174	-0.519
<i>E. ventermaculus</i> .GoO	<i>E. guttata</i> .GoO	0.607	0.231	1.018
<i>E. ventermaculus</i> .GoO	<i>H. fuscopinna</i> .GoO	0.152	-0.260	0.582
<i>E. ventermaculus</i> .GoO	<i>H. vulgaris</i> .GoO	1.307	0.895	1.691
<i>E. guttata</i> .GoO	<i>H. fuscopinna</i> .GoO	-0.453	-0.822	-0.088
<i>E. guttata</i> .GoO	<i>H. vulgaris</i> .GoO	0.700	0.360	1.041
<i>H. fuscopinna</i> .GoO	<i>H. vulgaris</i> .GoO	1.153	0.799	1.543

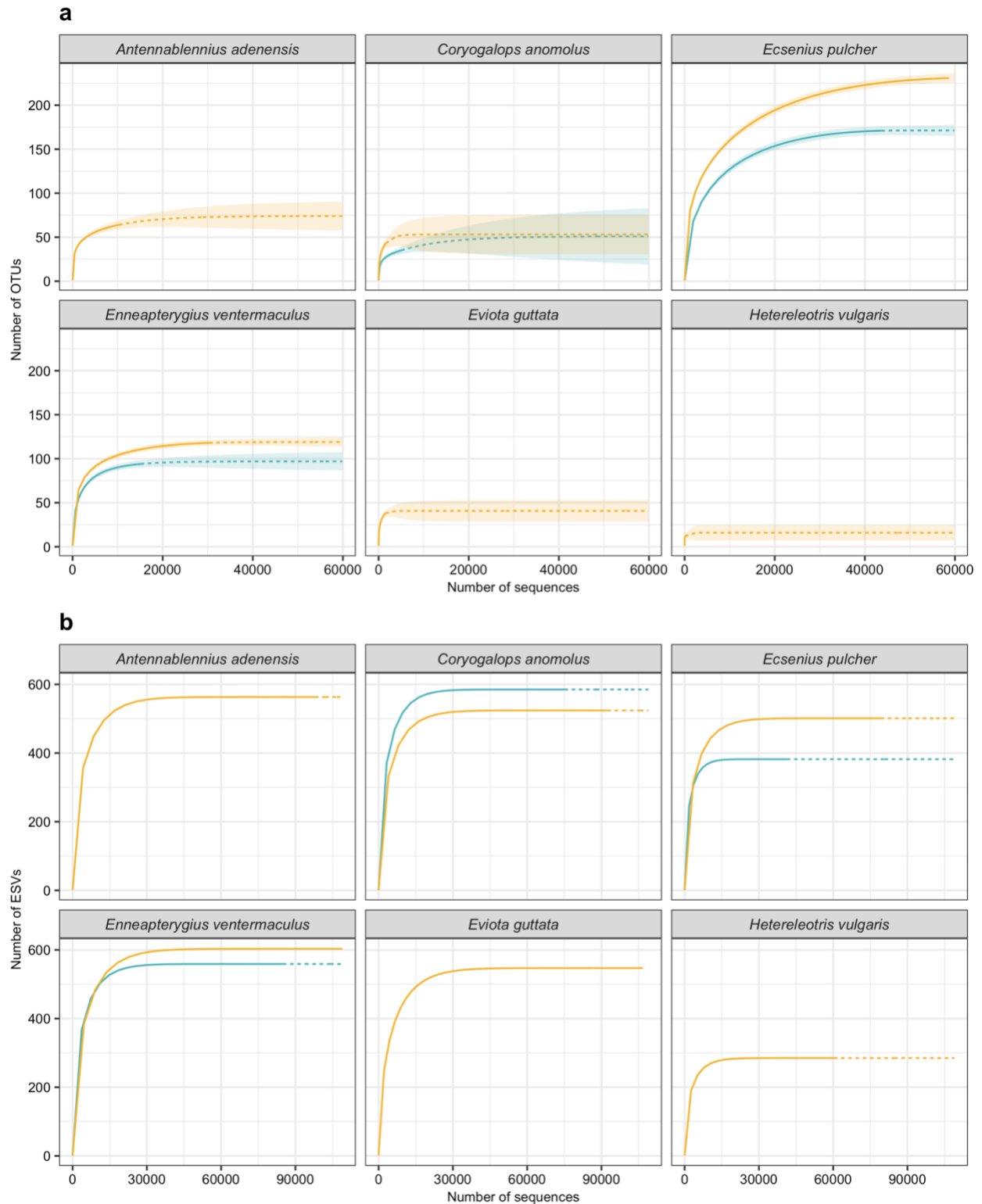


Figure S1 | Rarefaction curves of OTU and ESV richness across total sequences for six species in the Arabian Gulf (blue) and Gulf of Oman (gold). OTU curves (a) indicate the diversity of prey items for each species and population as obtained from gut

1136 content DNA metabarcoding with the COI marker, while ESV curves (b) show the
1137 diversity of prey items obtained with the 23S marker. Solid lines indicate interpolated
1138 richness, while dashed lines indicate extrapolated richness (to the maximum number of
1139 sequences across species). Shaded ribbons indicate 95% confidence intervals of
1140 extrapolations.
1141